

Approximate Asymptotic Distribution of Locally Most Powerful Invariant Test for Independence: Complex Case

Yu-Hang Xiao, *Student Member, IEEE*, Lei Huang, *Senior Member, IEEE*, Junhao Xie, *Senior Member, IEEE*, and Hing Cheung So, *Fellow, IEEE*

Abstract—Usually, it is very difficult to determine the *exact* distribution for a test statistic. In this paper, asymptotic distributions of locally most powerful invariant test for independence of complex Gaussian vectors are developed. In particular, its cumulative distribution function (CDF) under the null hypothesis is approximated by a function of chi-squared CDFs. Moreover, the CDF corresponding to the non-null distribution is expressed in terms of non-central chi-squared CDFs for close hypothesis, and Gaussian CDF as well as its derivatives for far hypothesis. The results turn out to be very accurate in terms of fitting their empirical counterparts. Closed-form expression for the detection threshold is also provided. Numerical results are presented to validate our theoretical findings.

Index Terms—Independence test, locally most powerful invariant test, asymptotic series expansion, chi-squared approximation, threshold calculation.

I. INTRODUCTION

VARIOUS practical problems can be cast as testing whether sets of random variables are mutually independent or not. As a result, testing for independence has inspired much research over the years. Among the extensive literature, the most classic topic is to detect the independence between a j -set and a k -set of random variables in a $(j+k)$ -variate Gaussian population [1]–[4]. This problem was generalised to the case of multiple sets in [5], where the generalized likelihood ratio test (GLRT), also called the Hadamard ratio test, was derived. The Hadamard ratio test is widely employed in numerous fields, such as spectrum sensing [6]–[8], multiple-channel signal detection [9], [10] and adaptive filtering [11].

Manuscript received September 15, 2016; revised January 5, 2017; accepted January 19, 2017. Date of publication February 14, 2017; date of current version February 15, 2018. The work described in this paper was supported in part by the National Natural Science Foundation of China under Grant U1501253, in part by the Natural Science Foundation of Guangdong Province under Grant 2015A030311030 and in part by the Foundation of Shenzhen Government under Grant ZDSYS201507081625213 and Grant KC2015ZDYF0023A.

Y.-H. Xiao and J. Xie are with Department of Electronic Engineering, Harbin Institute of Technology, Harbin 150001, China (e-mail: yuhangxiao@outlook.com; xj@hit.edu.cn).

L. Huang is with College of Information Engineering, Shenzhen University, Shenzhen, 518060, China (e-mail: dr.lei.huang@ieee.org).

H. C. So is with Department of Electronic Engineering, City University of Hong Kong, Hong Kong (e-mail: hcso@ee.cityu.edu.hk).

Communicated by P. Harremoës, Associate Editor for Probability and Statistics.

Color versions of one or more of the figures in this paper are available online at <http://ieeexplore.ieee.org>.

Digital Object Identifier 10.1109/TIT.2017.2669021

Since the Hadamard ratio test has its roots in the GLRT principle, it does not perform well particularly when the alternative hypothesis (\mathcal{H}_1) is near to the null hypothesis (\mathcal{H}_0), which corresponds to the most challenging real-world applications. For instance, the FCC regulations require reliable detection of primary signals with signal-to-noise ratio (SNR) as low as -18 dB [12]. To handle the issue of signal detection at very low SNRs, one needs to explore more efficient testing approaches. Indeed, Nagao [13] has devised an efficient detector based on the asymptotic variance of the Hadamard ratio test by replacing the unknown parameters with their maximum likelihood (ML) estimates, which is equivalent to the Frobenius norm of the sample correlation matrix. In the complex-valued case, Lesham and van der Veen [10] have used the Frobenius norm of the sample correlation matrix as an *ad hoc* detector for spectrum sensing. Recently, Ramírez *et al.* [14] have proved that this detector is exactly the locally most powerful invariant test (LMPIT) for testing independence of Gaussian vectors, which in turn indicates that it is optimal in the case of close hypothesis (low SNR scenario). On the other hand, a limiting distribution under null hypothesis has been addressed in [14]. Nevertheless, the accuracy of the limiting distribution considerably degrades as the sample size n becomes small. This is because the limiting distribution ignores the $\mathcal{O}(n^{-1})$ term, which is valid when n is large enough but not appropriate as n is relatively small. Under such conditions, the approximate formulae in [14] cannot offer accurate threshold computation for the LMPIT. As a matter of fact, an asymptotic series expansion can significantly improve the accuracy of the approximation over the limiting distribution for relatively small samples because the former considers the higher-order terms which have been omitted by the latter. Furthermore, the asymptotic series expansion usually results in a null distribution expressed as the sum of weighted chi-squared cumulative distribution functions (CDFs), which is invertible, thus producing a closed-form expression for threshold calculation. This in turn avoids numerically inverting the null distribution and offers computational simplicity in practical applications.

In the real-valued case, Nagao [13] has derived the asymptotic series expansions of the null distribution for the LMPIT by inverting the asymptotic formula of the characteristic function, which consists of the hypergeometric expressions with matrix argument. The accuracy of the asymptotic results

is up to $\mathcal{O}(n^{-2})$. Under the alternative hypothesis, however, the asymptotic series expansion usually fails to yield an accurate approximate distribution no matter if the alternative hypothesis is close to or far from the null hypothesis. This is due to the fact that the covariance matrix expansions are different under these two conditions [16], [17]. Since the LMPIT is inherently devised for signal detection in close hypothesis, it is of interest to determine its distribution in this scenario. Note that Nagao [18] has derived a noncentral Chi-squared approximation for the LMPIT under the close hypothesis in the real-valued Gaussian situation, whose remainder term is $\mathcal{O}(n^{-\frac{3}{2}})$. The close hypothesis [18] means that the elements of matrix $\mathbf{Z} \triangleq \sqrt{n}(\boldsymbol{\Sigma} - \mathbf{I}_p)$ are of order $\mathcal{O}(1)$, where $\boldsymbol{\Sigma}$ is the $p \times p$ covariance matrix and \mathbf{I}_p is the $p \times p$ identity matrix. In this work, the asymptotic series expansion method is applied to the complex Gaussian scenarios, where the real and imaginary parts are jointly Gaussian, that is, we extend the previous results [13], [18] to the complex-valued case. For far hypothesis, in which the elements of $\mathbf{Z}' \triangleq \boldsymbol{\Sigma} - \mathbf{I}_p$ are of order $\mathcal{O}(1)$, we have derived another accurate approximation which is expressed as the sum of weighted Gaussian distribution and its derivatives. The derived distributions turn out to be computationally simple and reasonably accurate, thereby enabling us to reliably predict the false-alarm and detection probabilities of the LMPIT. The theoretical results are advantageous over Monte Carlo simulation since the latter is computationally expensive. Furthermore, we obtain a closed-form formula that allows one to precisely set the threshold for a prescribed false-alarm rate. The simple expression of the decision threshold facilitates real-time processing in practical applications. It should be pointed out that our results rely on the assumption that p is much smaller than n . When p and n are comparable, their accuracy cannot be guaranteed. Under such circumstances, Mestre *et al.* [19] have derived the null and non-null distributions of the LMPIT for the complex scalar case via the central limit theorem (CLT). Note that the results in [19] are sufficiently precise only when both p and n are large and comparable in magnitude, thus being complementary with the results in this work.

The remainder of this paper is organized as follows. The LMPIT approach for signal detection is presented in Section II. In Section III, the asymptotic null distribution of the LMPIT is determined by inverting the asymptotic formula of its characteristic function. Based on the so-obtained distribution, we derive a simple and accurate analytical expression for threshold computation. Under the close and far hypotheses, the distribution is expanded up to $\mathcal{O}(n^{-\frac{3}{2}})$, which is presented in Sections IV and V. Section VI provides simulation results to confirm the theoretical calculations. Finally, conclusions are drawn in Section VII.

Throughout this paper, we use boldface uppercase letters for matrices, boldface lowercase letters for column vectors, and normal font letters for scalar quantities. The $\mathbb{E}[a]$ denotes the expected value of a . The $\mathbf{A} \in \mathbb{R}^{p \times q} (\mathbb{C}^{p \times q})$ means that \mathbf{A} is a $p \times q$ real (complex) matrix and \mathbf{A}_{ij} ($\mathbf{A}_{i,j}$) stands for the (i, j) block (entry) of \mathbf{A} . The $|\mathbf{A}|$, $\|\mathbf{A}\|_F$ and $\text{tr}(\mathbf{A})$ are the determinant, Frobenius norm and trace of \mathbf{A} , and

$\text{diag}(\mathbf{A}_{11}, \dots, \mathbf{A}_{qq})$ is a block-diagonal matrix formed by the matrices $\mathbf{A}_{11}, \dots, \mathbf{A}_{qq}$. Superscripts $(\cdot)^{-1}$, $(\cdot)^T$, $(\cdot)^H$ and $(\cdot)^*$ represent matrix inverse, transpose, Hermitian transpose and conjugate operations. The $\mathbf{0}_{p \times q}$ is the $p \times q$ zero matrix. The $\mathbf{x} \sim \mathcal{CN}(\boldsymbol{\mu}, \boldsymbol{\Sigma})$ means that \mathbf{x} follows a circular complex Gaussian distribution with mean $\boldsymbol{\mu}$ and covariance matrix $\boldsymbol{\Sigma}$, and \sim signifies ‘‘distributed as’’. When \mathbf{S} follows a complex Wishart distribution with n degrees-of-freedom (DOFs) and covariance matrix $\boldsymbol{\Sigma} \in \mathbb{C}^{p \times p}$, we write $\mathbf{S} \sim \mathcal{W}_p(n, \boldsymbol{\Sigma})$. The χ_f^2 and $\chi_f^2(\sigma^2)$ denote a central and non-central Chi-squared distributed random variable, respectively, where f is the DOFs and σ^2 is the noncentrality parameter. The $\mathbf{A}^{\frac{1}{2}}$ ($\mathbf{A}^{-\frac{1}{2}}$) is the Hermitian square root of the Hermitian matrix \mathbf{A} (\mathbf{A}^{-1}). In addition, the exponential function of any Hermitian matrix is defined as

$$e^{\mathbf{A}} = \mathbf{I} + \mathbf{A} + \frac{\mathbf{A}^2}{2!} + \frac{\mathbf{A}^3}{3!} + \dots + \frac{\mathbf{A}^n}{n!} + \dots \quad (1)$$

II. LMPIT APPROACH

Suppose $\mathbf{r} \in \mathbb{C}^{p \times 1}$ follows a circular complex Gaussian distribution $\mathcal{CN}(\mathbf{0}_{p \times 1}, \boldsymbol{\Sigma})$, which is partitioned into q sub-vectors with lengths p_1, \dots, p_q . That is,

$$\mathbf{r} = [\mathbf{r}_1^T, \mathbf{r}_2^T, \dots, \mathbf{r}_q^T]^T, \quad (2)$$

where $\mathbf{r}_j \in \mathbb{C}^{p_j \times 1}$, $j = 1, \dots, q$. Accordingly, the covariance matrix $\boldsymbol{\Sigma}$ is expressed as

$$\boldsymbol{\Sigma} = \mathbb{E}[\mathbf{r}\mathbf{r}^H] = \begin{bmatrix} \boldsymbol{\Sigma}_{11} & \boldsymbol{\Sigma}_{12} & \dots & \boldsymbol{\Sigma}_{1q} \\ \boldsymbol{\Sigma}_{21} & \boldsymbol{\Sigma}_{22} & \dots & \boldsymbol{\Sigma}_{2q} \\ \vdots & \vdots & \ddots & \vdots \\ \boldsymbol{\Sigma}_{q1} & \boldsymbol{\Sigma}_{q2} & \dots & \boldsymbol{\Sigma}_{qq} \end{bmatrix}, \quad (3)$$

with $\boldsymbol{\Sigma}_{jk} \in \mathbb{C}^{p_j \times p_k}$. Given n realizations of \mathbf{r} , say, $\mathbf{r}(1), \dots, \mathbf{r}(n)$, our aim is to test whether the sub-vectors $\mathbf{r}_1, \dots, \mathbf{r}_q$, are mutually independent. When the null hypothesis is true, this means that the corresponding covariance matrix $\boldsymbol{\Sigma}$ is block diagonal:

$$\boldsymbol{\Sigma} = \begin{bmatrix} \boldsymbol{\Sigma}_{11} & \mathbf{0}_{p_1 \times p_2} & \dots & \mathbf{0}_{p_1 \times p_q} \\ \mathbf{0}_{p_2 \times p_1} & \boldsymbol{\Sigma}_{22} & \dots & \mathbf{0}_{p_2 \times p_q} \\ \vdots & \vdots & \ddots & \vdots \\ \mathbf{0}_{p_q \times p_1} & \mathbf{0}_{p_q \times p_2} & \dots & \boldsymbol{\Sigma}_{qq} \end{bmatrix}. \quad (4)$$

Consequently, the binary hypothesis test¹

$$\mathcal{H}_0 : \boldsymbol{\Sigma} = \text{diag}(\boldsymbol{\Sigma}_{11}, \dots, \boldsymbol{\Sigma}_{qq}) \quad (5a)$$

$$\mathcal{H}_1 : \boldsymbol{\Sigma} \neq \text{diag}(\boldsymbol{\Sigma}_{11}, \dots, \boldsymbol{\Sigma}_{qq}). \quad (5b)$$

The LMPIT derived in [14] is given as

$$T_{\text{LMP}} = \|\mathbf{C}\|_F^2, \quad (6)$$

¹Note that the hypothesis testing model in (5) cannot be rewritten as a $2p$ -dimensional real-valued independence test, since the circularity of \mathbf{x} implies that its real and imaginary parts are identically distributed and could be correlated [15, eq. (14)], which contradicts with the null hypothesis model in the real-valued case.

where

$$\mathbf{C} = \mathbf{S}_D^{-\frac{1}{2}} \mathbf{S} \mathbf{S}_D^{-\frac{1}{2}}, \quad (7)$$

in which

$$\mathbf{S} = \sum_{j=1}^n \mathbf{r}(j) \mathbf{r}^H(j) \quad (8)$$

is the sample covariance matrix (SCM) and \mathbf{S}_D is defined as

$$\mathbf{S}_D = \text{diag}(\mathbf{S}_{11}, \dots, \mathbf{S}_{qq}). \quad (9)$$

Herein, \mathbf{S}_{jk} is defined in the same manner as Σ_{jk} .² It follows from [14] that the test variable $nT_{\text{LMP}} - np$ is asymptotically Chi-squared distributed. Therefore, for simplicity, its monotonic form is used instead, that is

$$T = n \text{tr}(\mathbf{S} \mathbf{S}_D^{-1} - \mathbf{I}_p)^2. \quad (10)$$

The hypothesis \mathcal{H}_0 is rejected when the test statistic T is larger than a given threshold γ , i.e.,

$$T \underset{\mathcal{H}_0}{\overset{\mathcal{H}_1}{\geq}} \gamma. \quad (11)$$

On the other hand, the limiting null distribution of the LMPIT has been approximated in [14] via that of the Hadamard ratio test, which could be obtained by the Wilks' theorem [20]. In particular, the approximation $\log|\mathbf{C}| \approx -\frac{1}{2} \text{tr}(\mathbf{C} - \mathbf{I}_p)^2$ is utilized in [14] to derive the limiting distribution of the LMPIT. However, this approximation is valid only for large sample scenario when \mathbf{C} approaches the identity matrix. For the small sample situation, the limiting distribution of the LMPIT in [14] is not accurate any more. On the other hand, the non-null distribution of the LMPIT has not yet been studied in the literature. In this work, we derive accurate null and non-null distributions for the LMPIT by means of inverting the asymptotic formula of the characteristic function of the LMPIT statistic.

III. NULL DISTRIBUTION

In this section, accurate expression for the asymptotic null distribution of T is determined by inverting the asymptotic formula of its characteristic function, which turns out to be a special case of the general result derived in Section IV. Moreover, closed-form formula for threshold calculation is produced.

Note that the distributions of the test statistic T are identical under population covariance matrices Σ and $\Sigma_D^{-1/2} \Sigma \Sigma_D^{-1/2}$. Without loss of generality, we assume $\Sigma = \mathbf{I}_p$ under the null hypothesis. As a result, it follows from [21] that $\mathbf{S} \sim \mathcal{W}_p(n, \mathbf{I}_p)$ with probability density function (PDF) of

$$f_{\mathbf{S}}(\mathbf{S}|\mathcal{H}_0) = \frac{1}{\Gamma_p(n)} |\mathbf{S}|^{n-p} \text{etr}(-\mathbf{S}), \quad (12)$$

where $\text{etr}(\cdot)$ stands for $\exp(\text{tr}(\cdot))$. To alleviate the difficulty in the derivation of the asymptotic distribution of T , we use

²In the following context, we use the subscript $(\cdot)_D$ to represent the same operation as $\mathbf{S} \rightarrow \mathbf{S}_D$.

the logarithm of \mathbf{S} , i.e., $\mathbf{Y} \triangleq \sqrt{n} \log(\mathbf{S}/n)$. It is shown in Appendix A that the asymptotic distribution of \mathbf{Y} is

$$f_{\mathbf{Y}}(\mathbf{Y}|\mathcal{H}_0) = c_1 \times \text{etr} \left(-\frac{\mathbf{Y}^2}{2} \right) \left[1 - \frac{\text{tr}(\mathbf{Y}^3)}{6\sqrt{n}} + \frac{p \text{tr}(\mathbf{Y}^2)}{12n} - \frac{\text{tr}^2(\mathbf{Y})}{12n} - \frac{\text{tr}(\mathbf{Y}^4)}{24n} + \frac{\text{tr}^2(\mathbf{Y}^3)}{72n} + \mathcal{O}(n^{-\frac{3}{2}}) \right], \quad (13)$$

where

$$c_1 = \frac{N^{p(N-\frac{p}{2})} \pi^{-\frac{p(p-1)}{2}} \exp(-np)}{\prod_{k=1}^p (\Gamma(n+1-k))}. \quad (14)$$

On the other hand, it is demonstrated in Appendix B that T can be expressed in terms of \mathbf{Y} as

$$T = f_0(\mathbf{Y}) + \frac{1}{\sqrt{n}} f_1(\mathbf{Y}) + \frac{1}{n} f_2(\mathbf{Y}) + \mathcal{O}(n^{-\frac{3}{2}}), \quad (15)$$

where

$$f_0(\mathbf{Y}) = \text{tr}(\mathbf{Y}^2 - \mathbf{Y}_D^2) \quad (16a)$$

$$f_1(\mathbf{Y}) = \text{tr} \left[2\mathbf{Y}_D^3 - 3\mathbf{Y}^2 \mathbf{Y}_D + \mathbf{Y}^3 \right] \quad (16b)$$

$$f_2(\mathbf{Y}) = \text{tr} \left[-\frac{7}{3} \mathbf{Y}_D \mathbf{Y}^3 + \frac{7}{12} \mathbf{Y}^4 + 5\mathbf{Y}^2 \mathbf{Y}_D^2 + (\mathbf{Y} \mathbf{Y}_D)^2 - \frac{5}{4} (\mathbf{Y}^2)_D^2 - 3\mathbf{Y}_D^4 \right]. \quad (16c)$$

Using (13) and (15), the characteristic function of T is written as

$$\begin{aligned} C(t) &= \mathbb{E}[\exp(\iota T)] \\ &= c \int \exp \left(-\frac{1}{2} \text{tr}(\mathbf{Y}^2) + (\iota t) f_0(\mathbf{Y}) \right) \times \left[1 + \frac{(\iota t)}{\sqrt{n}} f_1(\mathbf{Y}) \right. \\ &\quad \left. + \frac{1}{n} \left\{ \frac{p \text{tr}(\mathbf{Y}^2)}{12} - \frac{\text{tr}^2(\mathbf{Y})}{12} - \frac{\text{tr}(\mathbf{Y}^4)}{24} + (\iota t) f_2(\mathbf{Y}) \right. \right. \\ &\quad \left. \left. + \frac{1}{2} \left((\iota t) f_1(\mathbf{Y}) - \frac{\text{tr}(\mathbf{Y}^3)}{6} \right)^2 \right\} + \mathcal{O}(n^{-\frac{3}{2}}) \right] d\mathbf{Y}, \quad (17) \end{aligned}$$

where $\iota = \sqrt{-1}$ and the integration is carried out over the group of all $p \times p$ Hermitian matrices. As \mathbf{Y} is a $p \times p$ Hermitian matrix, it has p^2 free parameters, i.e., $\mathbf{Y}_{1,1}, \mathbf{Y}_{2,2}, \dots, \mathbf{Y}_{p,p}, \mathbf{Y}_{1,2}^R, \mathbf{Y}_{1,3}^R, \dots, \mathbf{Y}_{p-1,p}^R, \mathbf{Y}_{1,2}^I, \mathbf{Y}_{1,3}^I, \dots, \mathbf{Y}_{p-1,p}^I$, where $\mathbf{Y}_{j,k}^R$ and $\mathbf{Y}_{j,k}^I$ denote the real and imaginary parts of $\mathbf{Y}_{j,k}$ ($j < k$), respectively. Furthermore, the exponential term in (17) can be unfolded as

$$\begin{aligned} &\exp \left(-\frac{1}{2} \text{tr}(\mathbf{Y}^2) + (\iota t) f_0(\mathbf{Y}) \right) \\ &= \exp \left(-\frac{1}{2} (1 - 2\iota t) \text{tr} \left(\mathbf{Y}^2 + \frac{2\iota t}{1 - 2\iota t} \mathbf{Y}_D^2 \right) \right) \\ &= \prod_{j=1}^p \exp \left(-\frac{\mathbf{Y}_{j,j}^2}{2v_{j,j}} \right) \prod_{\substack{j,k=1 \\ j < k}}^p \exp \left(-\frac{(\mathbf{Y}_{j,k}^R)^2}{2v_{j,k}} \right) \exp \left(-\frac{(\mathbf{Y}_{j,k}^I)^2}{2v_{j,k}} \right), \quad (18) \end{aligned}$$

where

$$v_{j,j} \triangleq 1 \quad j = 1, \dots, p \quad (19a)$$

$$v_{j,k} \triangleq \frac{1}{2(1 - 2it + 2it\delta_{\alpha(j)\alpha(k)})} \quad j, k = 1, \dots, p, \quad j < k, \quad (19b)$$

in which δ_{ab} represents the Kronecker delta function and $\alpha(j)$ is the integer such that

$$\sum_{s=1}^{\alpha(j)-1} p_s < j \leq \sum_{s=1}^{\alpha(j)} p_s. \quad (20)$$

It is observed that the right-hand side (RHS) of (18) can be taken as a product of Gaussian PDFs (dropping the constant terms), enlightening us to utilize the following integration:

$$\int_{-\infty}^{\infty} x^k \underbrace{\frac{1}{\sqrt{2\pi v}} \exp\left[-\frac{x^2}{2v}\right]}_{\text{Gaussian PDF}} dx = \begin{cases} 0 & \text{if } k \text{ is odd} \\ v^{\frac{k}{2}}(k-1)!! & \text{if } k \text{ is even,} \end{cases} \quad (21)$$

which holds when v is a positive real number or a complex number with positive real part. Therefore, the characteristic function in (17) can be adopted as:

$$\begin{aligned} C(t) = & c_2 \times \phi^{\frac{f}{2}} \mathbb{E} \left[1 + \frac{(it)}{\sqrt{n}} f_1(\mathbf{Y}') \right. \\ & + \frac{1}{n} \left\{ \frac{\text{ptr}(\mathbf{Y}'^2)}{12} - \frac{\text{tr}^2(\mathbf{Y}')}{12} - \frac{\text{tr}(\mathbf{Y}'^4)}{24} + (it) f_2(\mathbf{Y}') \right. \\ & \left. \left. + \frac{1}{2} \left((it) f_1(\mathbf{Y}') - \frac{\text{tr}(\mathbf{Y}'^3)}{6} \right)^2 \right\} + \mathcal{O}(n^{-\frac{3}{2}}) \right], \quad (22) \end{aligned}$$

where $f = p^2 - \sum_{i=1}^q p_i^2$, $\phi = (1 - 2it)^{-1}$, $c_2 = c_1 \times (2\pi)^{\frac{p^2}{2}} 2^{-\frac{p(p-1)}{2}}$ and the mathematical expectation is calculated with respect to the $p \times p$ matrix \mathbf{Y}' , whose elements are defined as

$$\mathbf{Y}'_{j,j} = \sqrt{v_{j,j}} u_{j,j} \quad j = 1, \dots, p \quad (23a)$$

$$\mathbf{Y}'_{j,k} = \mathbf{Y}'_{j,k}^R + i \mathbf{Y}'_{j,k}^I \quad j, k = 1, \dots, p, \quad j < k \quad (23b)$$

$$\mathbf{Y}'_{k,j} = \mathbf{Y}'_{j,k}^R - i \mathbf{Y}'_{j,k}^I \quad j, k = 1, \dots, p, \quad j < k, \quad (23c)$$

where

$$\mathbf{Y}'_{j,k}^R = \sqrt{v_{j,k}} u_{j,k}^R \quad j, k = 1, \dots, p, \quad j < k \quad (24a)$$

$$\mathbf{Y}'_{j,k}^I = \sqrt{v_{j,k}} u_{j,k}^I \quad j, k = 1, \dots, p, \quad j < k \quad (24b)$$

with $u_{j,j}$, $u_{j,k}^R$ and $u_{j,k}^I$ being mutually independent Gaussian variables with mean 0 and variance 1. Subsequently, the moments corresponding to (22) can be calculated using (23) and (24), which are shown in Table III of Appendix C.

Notice that the distribution function is monotonic and has the upper and lower bounds of 0 and 1, which indicates that (22) equals 1 at $t = 0$. Unfortunately, an asymptotic series expansion including c_2 does not provide this property. To circumvent this issue, we need to replace the constant factor c_2 with its Stirling's approximation:

$$c_2 = 1 - \frac{2p^3 - p}{12n} + \mathcal{O}(n^{-2}). \quad (25)$$

The derivation of (25) is given in Appendix D. Note that this replacement does not have an influence on the order of the remainder term in the asymptotic series expansion. Substituting the so-obtained moments in Table III along with (25) into (22) yields the asymptotic expression of the characteristic function

$$C(t) = \phi^{\frac{f}{2}} \left[\sum_{k=0}^3 h_k \phi^k + \mathcal{O}(n^{-2}) \right], \quad (26)$$

where

$$h_0 = 1 + \frac{-p^3 + \tilde{p}_3}{6n} \quad (27a)$$

$$h_1 = \frac{p^3 - p\tilde{p}_2}{2n} \quad (27b)$$

$$h_2 = \frac{-p^3 - \tilde{p}_3 + 2p\tilde{p}_2}{2n} \quad (27c)$$

$$h_3 = \frac{p^3 + 2\tilde{p}_3 - 3p\tilde{p}_2}{6n} \quad (27d)$$

with $\tilde{p}_k = \sum_{j=1}^q p_j^k$. Note that the order of remainder terms reduces to $\mathcal{O}(n^{-2})$ due to the fact that the odd moments of \mathbf{Y}' equal zero. Inverting the characteristic function, we have the following result.

Theorem 1: Under the null hypothesis, the CDF of T is approximated asymptotically up to $\mathcal{O}(n^{-2})$ by

$$\Pr(T \leq \gamma) = \sum_{k=0}^3 h_k \Pr(\chi_{f+2k}^2 \leq \gamma) + \mathcal{O}(n^{-2}). \quad (28)$$

Inversely, for a given false-alarm probability P_{fa} , the theoretical threshold is determined as

$$1 - P_{fa} = \Pr(T \leq \gamma). \quad (29)$$

To proceed, the following result [13], [22] is needed.

Lemma 1: If the null distribution of a test statistic ε has the following expansion

$$\Pr(\varepsilon \leq \gamma) = \Pr(\chi_f^2 \leq \gamma) + \frac{1}{n} \sum_{k=0}^3 \beta_k \Pr(\chi_{f+2k}^2 \leq \gamma) + \mathcal{O}(n^{-2}) \quad (30)$$

with $\sum_{k=0}^3 \beta_k = 0$, then the asymptotic formula for its 100a% point is

$$\begin{aligned} \gamma(P_{fa}) = & u + \frac{1}{n} \left\{ \frac{2\beta_3 u}{f(f+2)(f+4)} \left[u^2 + (f+4)u \right. \right. \\ & \left. \left. + (f+2)(f+4) \right] + \frac{2\beta_2 u}{f(f+2)} (u+f+2) + \frac{2\beta_1 u}{f} \right\} \\ & + \mathcal{O}(n^{-2}), \quad (31) \end{aligned}$$

where $\Pr(\chi_f^2 \geq u) = a$.

Applying this lemma, it is easy to obtain the expression of decision threshold for any given P_{fa} , that is

$$\begin{aligned} \gamma(P_{fa}) = & u + \frac{2h_3 u}{f(f+2)(f+4)} \left[u^2 + (f+4)u \right. \\ & \left. + (f+2)(f+4) \right] + \frac{2h_2 u}{f(f+2)} (u+f+2) + \frac{2h_1 u}{f} \\ & + \mathcal{O}(n^{-2}), \quad (32) \end{aligned}$$

where $\Pr(\chi_f^2 \geq u) = 1 - P_{fa}$.

It should be pointed out that although the asymptotic distribution is the sum of weighted Chi-squared CDFs with different DOFs, the threshold can still be expressed in terms of $100(1 - P_{\text{fa}})\%$ point of the Chi-squared distribution with DOF f , thereby avoiding the numerical evaluation of (29). Hence, the computational cost in the theoretical threshold calculation is very low.

IV. NON-NULL DISTRIBUTION UNDER CLOSE HYPOTHESIS

In this section, the non-null distribution of T under close hypothesis is derived in terms of noncentral Chi-squared distributions, which can be used to determine the approximate detection probability (P_d). Similar to our argument in Section III, we assume $\Sigma_D = \mathbf{I}_p$ without loss of generality. Following [16]–[18], the alternative hypothesis can be considered as “close” to the null hypothesis when the non-zero elements of $(\Sigma - \mathbf{I}_p)$ are of order $\mathcal{O}(1/\sqrt{n})$.

Under the alternative hypothesis, \mathbf{S} follows a correlated complex Wishart distribution $\mathcal{W}_p(n, \Sigma)$ with density

$$f_{\mathbf{S}}(\mathbf{S}|\mathcal{H}_1) = \frac{1}{\Gamma_p(n)|\Sigma|^n} |\mathbf{S}|^{n-p} \text{etr}(-\mathbf{S}\Sigma^{-1}). \quad (33)$$

Applying the similar manipulations used in Appendix A, the asymptotic distribution of \mathbf{Y} under the close hypothesis is calculated as

$$f_{\mathbf{Y}}(\mathbf{Y}|\mathcal{H}_1) = c_1 \times \text{etr}(s_0) \times \left[1 + \frac{s_1(\mathbf{Y})}{\sqrt{n}} + \frac{s_2(\mathbf{Y})}{n} + \frac{s_1^2(\mathbf{Y})}{2n} + \mathcal{O}(n^{-\frac{3}{2}}) \right], \quad (34)$$

where

$$s_0(\mathbf{Y}) = -\frac{\mathbf{Y}^2}{2} + \mathbf{Y}\mathbf{Z} - \frac{\mathbf{Z}^2}{2} \quad (35a)$$

$$s_1(\mathbf{Y}) = -\frac{\mathbf{Y}^3}{6} - \mathbf{Z}^2\mathbf{Y} + \frac{\mathbf{Z}\mathbf{Y}^2}{2} + \frac{2\text{tr}(\mathbf{Z}^3)}{3} \quad (35b)$$

$$s_2(\mathbf{Y}) = \frac{p\text{tr}(\mathbf{Y}^2)}{12} - \frac{\text{tr}^2(\mathbf{Y})}{12} - \frac{\mathbf{Y}^4}{24} - \frac{\mathbf{Y}^2\mathbf{Z}^2}{2} + \frac{\mathbf{Y}^3\mathbf{Z}}{6} + \mathbf{Y}\mathbf{Z}^3 - \frac{3\text{tr}(\mathbf{Z}^4)}{4} \quad (35c)$$

with

$$\mathbf{Z} \triangleq \sqrt{n}(\Sigma - \mathbf{I}_p). \quad (36)$$

It follows that the characteristic function of T is

$$C(t) = c \int \exp(s_0(\mathbf{Y}) + (it)f_0(\mathbf{Y})) \times \left[1 + \frac{1}{\sqrt{n}}(s_1(\mathbf{Y}) + (it)f_1(\mathbf{Y})) + \frac{1}{n} \left\{ (it)f_2(\mathbf{Y}) + s_2(\mathbf{Y}) + \frac{1}{2}(s_1(\mathbf{Y}) + (it)f_1(\mathbf{Y}))^2 \right\} + \mathcal{O}(n^{-\frac{3}{2}}) \right] d\mathbf{Y}, \quad (37)$$

where

$$\exp(s_0(\mathbf{Y}) + (it)f_0(\mathbf{Y})) = \exp\left(-\frac{1}{2\phi} \left[\text{tr}(\mathbf{Y} - \phi\mathbf{Z})^2 + 2it\phi \text{tr}((\mathbf{Y} - \phi\mathbf{Z})_D^2) \right]\right). \quad (38)$$

Similar to our arguments in (17)–(22), the exponential function of \mathbf{Y} can be seen as a product of Gaussian PDFs, facilitating our computation of the integration in (37). Consequently, $C(t)$ is expressed as

$$C(t) = c_2 \times \phi^{\frac{f}{2}} \mathbb{E} \left[1 + \frac{1}{\sqrt{n}}(s_1(\mathbf{Y}'') + (it)f_1(\mathbf{Y}'')) + \frac{1}{n} \left\{ s_2(\mathbf{Y}'') + (it)f_2(\mathbf{Y}'') + \frac{1}{2}(s_1(\mathbf{Y}'') + (it)f_1(\mathbf{Y}''))^2 \right\} + \mathcal{O}(n^{-\frac{3}{2}}) \right], \quad (39)$$

in which the mathematical expectation is computed with respect to \mathbf{Y}'' , defined as $\mathbf{Y}'' = \mathbf{Y}' + \mathbf{Z}\phi$. Furthermore, the moments involved in (39) are listed in Table IV of Appendix C. Thus, the characteristic function is calculated as:

$$C(t) = \phi^{\frac{f}{2}} \exp((it)a_2\phi) \left[\sum_{k=0}^6 g_k \phi^k + \mathcal{O}(n^{-\frac{3}{2}}) \right], \quad (40)$$

where

$$g_0 = 1 + \frac{2a_3}{3\sqrt{n}} + \frac{2a_3^2}{9n} - \frac{3a_4}{4n} + \frac{b}{2n} + \frac{-p^3 + \tilde{p}_3}{6n} \quad (41a)$$

$$g_1 = -\frac{a_3}{\sqrt{n}} - \frac{2a_3^2}{3n} + \frac{3a_4}{2n} - \frac{3b}{2n} + \frac{p^3 - p\tilde{p}_2}{2n} \quad (41b)$$

$$g_2 = \frac{a_3^2}{2n} + \frac{pa_2}{2n} + \frac{b}{2n} + \frac{-p^3 - \tilde{p}_3 + 2p\tilde{p}_2}{2n} \quad (41c)$$

$$g_3 = \frac{a_3}{3\sqrt{n}} + \frac{2a_3^2}{9n} - \frac{a_4}{n} - \frac{pa_2}{n} + \frac{b}{n} + \frac{c}{n} + \frac{p^3 + 2\tilde{p}_3 - 3p\tilde{p}_2}{6n} \quad (41d)$$

$$g_4 = -\frac{a_3^2}{3n} - \frac{a_4}{4n} + \frac{pa_2}{2n} - \frac{c}{n} \quad (41e)$$

$$g_5 = \frac{a_4}{2n} - \frac{b}{2n} \quad (41f)$$

$$g_6 = \frac{a_3^2}{18n} \quad (41g)$$

with $a_j = \text{tr}(\mathbf{Z}^j)$, $b = \text{tr}((\mathbf{Z}^2)_D^2)$ and $c = \sum_{j,k=1}^p p_j \text{tr}(\mathbf{Z}_{jk}\mathbf{Z}_{kj})$. Inverting this characteristic function, the following theorem is obtained.

Theorem 2: Under close hypothesis that $(\Sigma - \mathbf{I}_p)$ is of order $\mathcal{O}(n^{-\frac{1}{2}})$, the CDF of T is approximated asymptotically up to $\mathcal{O}(n^{-\frac{3}{2}})$ by

$$\Pr(T \leq \gamma) = \sum_{k=0}^6 g_k \Pr(\chi_{f+2k}^2(\sigma^2) \leq \gamma) + \mathcal{O}(n^{-\frac{3}{2}}) \quad (42)$$

with $\sigma^2 = a_2/3$.

It should be noted that if we set Σ to the identity matrix, the same asymptotic series expansion of the null distribution as (28) can be obtained.

V. NON-NULL DISTRIBUTION UNDER FAR HYPOTHESIS

Under sufficiently high SNR conditions, the assumption of close hypothesis becomes invalid. Therefore, it is necessary to consider the situation when the alternative hypothesis is not

³Note that the noncentrality parameter $\sigma^2 = a_2/4$ in [18] should be corrected as $\sigma^2 = a_2/2$.

that close to the null hypothesis. For this situation, we assume that the non-zero elements of $(\boldsymbol{\Sigma} - \mathbf{I}_p)$ are of order $\mathcal{O}(1)$ and define:

$$\mathbf{Z}' \triangleq \boldsymbol{\Sigma} - \mathbf{I}_p \quad (43)$$

$$\mathbf{X} \triangleq \frac{\mathbf{S} - n\boldsymbol{\Sigma}}{\sqrt{n}}. \quad (44)$$

Accordingly, the asymptotic expansion of T under this setting can be expressed as (see Appendix B):

$$T = n\text{tr}(\mathbf{Z}'^2) + \sqrt{n}q_0(\mathbf{X}) + q_1(\mathbf{X}) + \frac{1}{\sqrt{n}}q_2(\mathbf{X}) + \mathcal{O}(n^{-1}), \quad (45)$$

where

$$q_0(\mathbf{X}) = \text{tr}[2\mathbf{Z}'(\mathbf{X} - \boldsymbol{\Sigma}\mathbf{X}_D)] \quad (46a)$$

$$q_1(\mathbf{X}) = \text{tr}[2\mathbf{Z}'(\boldsymbol{\Sigma}(\mathbf{X}_D)^2 - \mathbf{X}\mathbf{X}_D) + (\mathbf{X} - \boldsymbol{\Sigma}\mathbf{X}_D)^2] \quad (46b)$$

$$q_2(\mathbf{X}) = \text{tr}[2(\mathbf{X} - \boldsymbol{\Sigma}\mathbf{X}_D)(\boldsymbol{\Sigma}(\mathbf{X}_D)^2 - \mathbf{X}\mathbf{X}_D) + 2\mathbf{Z}'(\mathbf{X}(\mathbf{X}_D)^2 - \boldsymbol{\Sigma}(\mathbf{X}_D)^3)]. \quad (46c)$$

Furthermore, setting $T' = (T - n\text{tr}(\mathbf{Z}'^2))/\sqrt{n}$, the characteristic function of T' has the form of

$$C'(t) = \mathbb{E} \left[\exp((it)q_0(\mathbf{X})) \left\{ 1 + \frac{(it)}{\sqrt{n}}q_1(\mathbf{X}) + \frac{1}{n}((it)q_2(\mathbf{X}) + \frac{1}{2}(it)^2q_1^2(\mathbf{X})) + \mathcal{O}(n^{-\frac{3}{2}}) \right\} \right]. \quad (47)$$

Expressing $q_0(\mathbf{X})$ and $q_1(\mathbf{X})$ in terms of \mathbf{S} , we have

$$q_0(\mathbf{X}) = \frac{1}{\sqrt{n}}\text{tr}(\mathbf{B}\mathbf{S}) \quad (48a)$$

$$q_1(\mathbf{X}) = \frac{1}{n}\text{tr}[\mathbf{S}^2 - 2\boldsymbol{\Sigma}\mathbf{S}_D\mathbf{S} + (\boldsymbol{\Sigma}\mathbf{S}_D)^2 - 2\mathbf{Z}'\mathbf{S}\mathbf{S}_D + 2\mathbf{Z}'\boldsymbol{\Sigma}(\mathbf{S}_D)^2 + 2n\mathbf{Z}'\mathbf{S} - 2n\mathbf{Z}'\boldsymbol{\Sigma}\mathbf{S}_D], \quad (48b)$$

where $\mathbf{B} = 2[\mathbf{Z}' - (\mathbf{Z}'^2)_D]$. Since \mathbf{B} is Hermitian, it follows from [21, eq. (5.10)] that the first term in (47) can be determined as:

$$\begin{aligned} & \mathbb{E} \left[\exp((it)q_0(\mathbf{X})) \right] \\ &= \int \frac{1}{\pi^n |\boldsymbol{\Sigma}|^n} \exp\left(-\sum_{j=1}^n \mathbf{r}(j)^H \Psi^{-1} \mathbf{r}(j)\right) d\mathbf{R} \\ &= |\Psi \boldsymbol{\Sigma}^{-1}|^n, \end{aligned} \quad (49)$$

where $\Psi = (\boldsymbol{\Sigma}^{-1} - \frac{(it)}{\sqrt{n}}\mathbf{B})^{-1}$ and $\mathbf{R} = [\mathbf{r}(1), \dots, \mathbf{r}(n)]$. Using $|\mathbf{e}^{\mathbf{A}}| = \text{etr}(\mathbf{A})$, which holds for arbitrary square matrix \mathbf{A} , the determinant term in (49) can be further expanded as:

$$\begin{aligned} |\Psi \boldsymbol{\Sigma}^{-1}|^n &= \mathbf{I}_p - \frac{(it)}{\sqrt{n}}\mathbf{A} |^{-n} \\ &= \exp\left(\frac{(it)^2 \text{tr}(\mathbf{A}^2)}{2}\right) \times \left[1 + \frac{(it)^3}{3\sqrt{n}}\text{tr}(\mathbf{A}^3) \right. \\ &\quad \left. + \frac{1}{n} \left(\frac{(it)^4}{4}\text{tr}(\mathbf{A}^4) + \frac{(it)^6}{18}\text{tr}^2(\mathbf{A}^3) \right) + \mathcal{O}(n^{-\frac{3}{2}}) \right], \end{aligned} \quad (50)$$

where $\mathbf{A} = \mathbf{Q}\mathbf{B}\mathbf{Q}$ and $\mathbf{Q} = \boldsymbol{\Sigma}^{1/2}$. Moreover, similar to (49), we have

$$\begin{aligned} & \mathbb{E} \left[\exp((it)q_0(\mathbf{X})) \mathbf{S}_{r,s} \mathbf{S}_{k,l} \right] \\ &= \int \frac{1}{\pi^n |\boldsymbol{\Sigma}|^n} \exp\left(-\sum_{j=1}^n \mathbf{r}(j)^H \Psi^{-1} \mathbf{r}(j)\right) \\ &\quad \times \sum_{x,y=1}^n \mathbf{R}_{x,r}^* \mathbf{R}_{x,s} \mathbf{R}_{y,k}^* \mathbf{R}_{y,l} d\mathbf{R} \\ &= |\Psi \boldsymbol{\Sigma}^{-1}|^n \sum_{x,y=1}^n (\Psi_{r,s} \Psi_{k,l} + \sigma_{xy} \Psi_{k,s} \Psi_{r,l}) \\ &= |\Psi \boldsymbol{\Sigma}^{-1}|^n (n^2 \Psi_{r,s} \Psi_{k,l} + n \Psi_{k,s} \Psi_{r,l}). \end{aligned} \quad (51)$$

As the second term of (47) is of order $\mathcal{O}(n^{-\frac{1}{2}})$, we only need to expand its expectation up to $\mathcal{O}(n^{-\frac{1}{2}})$. Using (51), the expectation of the second term of (47) is computed in Appendix E, which is given as

$$\begin{aligned} & \mathbb{E}[q_1(\mathbf{X}) \exp((it)q_0(\mathbf{X}))] \\ &= \exp\left(\frac{(it)^2 \text{tr}(\mathbf{A}^2)}{2}\right) \times \left[d_0 + (it)^2 d_2 \right. \\ &\quad \left. + \frac{1}{\sqrt{n}} \left\{ (it)d_1 + (it)^3 d_3 + (it)^5 d_5 \right\} \right] + \mathcal{O}(n^{-1}), \end{aligned} \quad (52)$$

where d_0, \dots, d_5 are defined in Appendix E.

Similarly, for the n^{-1} terms in (47), we only need to explicitly compute the dominant terms of their expectations. To proceed, we define a new matrix $\mathbf{W} = \mathbf{Q}^{-1}\mathbf{X}\mathbf{Q}^{-1}$. It follows from the Berry–Esseen theorem [23], [24] that \mathbf{W} obeys an asymptotic distribution as

$$f(\mathbf{W}) = c_3 \times \exp\left(-\frac{1}{2}\text{tr}(\mathbf{W}^2)\right) + \mathcal{O}(n^{-\frac{1}{2}}), \quad (53)$$

with $c_3 = 1/(\pi^{p^2/2} 2^{p/2})$. Therefore, we have,

$$\begin{aligned} & \mathbb{E} \left[\exp((it)q_0(\mathbf{X})) (q_2(\mathbf{X}) + \frac{1}{2}q_1^2(\mathbf{X})) \right] \\ &= c_3 \times \text{etr}\left(\frac{(it)^2}{2}\mathbf{A}^2\right) \int \text{etr}\left[-\frac{1}{2}(\mathbf{W} - (it)\mathbf{A})^2\right] \\ &\quad \times (q_2(\mathbf{X}) + \frac{1}{2}q_1^2(\mathbf{X})) d\mathbf{W} + \mathcal{O}(n^{-\frac{1}{2}}). \end{aligned} \quad (54)$$

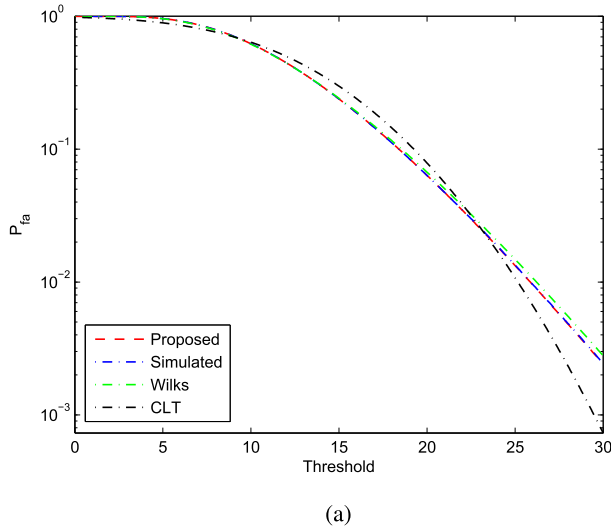
Utilizing the similar manipulations as Section III, we could take the term $\text{etr}[-1/2(\mathbf{W} - (it)\mathbf{A})^2]$ as a product of p^2 Gaussian PDFs, leading to

$$\begin{aligned} & c_3 \int \text{etr}\left[-\frac{1}{2}(\mathbf{W} - (it)\mathbf{A})^2\right] (q_2(\mathbf{X}) + \frac{1}{2}q_1^2(\mathbf{X})) d\mathbf{W} \\ &= \mathbb{E} \left[(it)q_2(\mathbf{X}') + \frac{(it)^2}{2}q_1(\mathbf{X}')^2 \right]. \end{aligned} \quad (55)$$

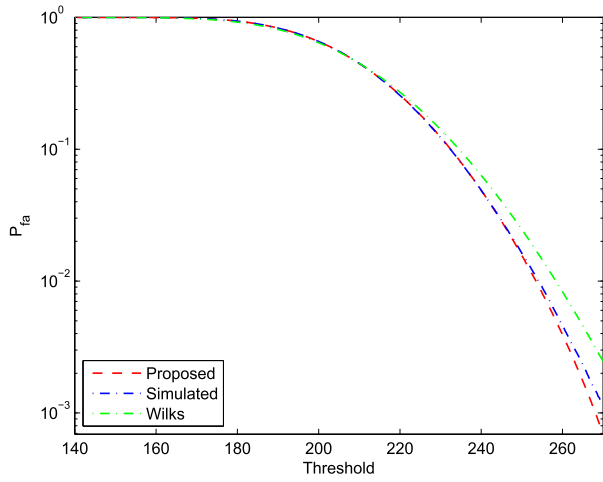
The mathematical expectation on the RHS of (55) is taken with respect to $\mathbf{X}' = \mathbf{Q}(\mathbf{W}' + it\mathbf{A})\mathbf{Q}$, where the elements of the $p \times p$ Hermitian matrix \mathbf{W}' are defined as

$$\mathbf{W}'_{j,j} = u_{j,j} \quad j = 1, \dots, p \quad (56a)$$

$$\mathbf{W}'_{j,k} = \frac{\sqrt{2}}{2} (u_{j,k}^R + it u_{j,k}^I) \quad j, k = 1, \dots, p, \quad j < k, \quad (56b)$$



(a)



(b)

Fig. 1. False-alarm probability versus threshold for different parameter settings. (a) $[p_1, p_2, p_3, p_4] = [1, 1, 1, 1]$, $n = 50$. (b) $[p_1, p_2, p_3] = [4, 6, 8]$, $n = 80$.

TABLE I
APPROXIMATION ERRORS OF FALSE-ALARM PROBABILITY

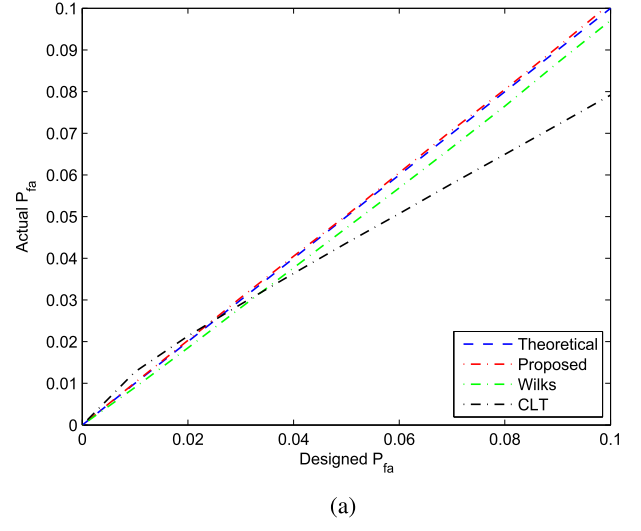
$[p_1, \dots, p_q]$	n	Wilks	Proposed	CLT
$[1, 1, 1, 1]$	50	9.9882×10^{-6}	3.9912×10^{-8}	1.414×10^{-3}
$[4, 6, 8]$	80	1.3550×10^{-4}	5.9757×10^{-7}	--

where $u_{j,j}$, $u_{j,k}^R$ and $u_{j,k}^I$ have been defined after (24) in Section III. Furthermore, the moments involved in (55) are listed in Tables V and VI of Appendix E. According to the so-obtained moments, the expectations of $q_2(\mathbf{X}')$ and $q_1^2(\mathbf{X}')$ are determined as

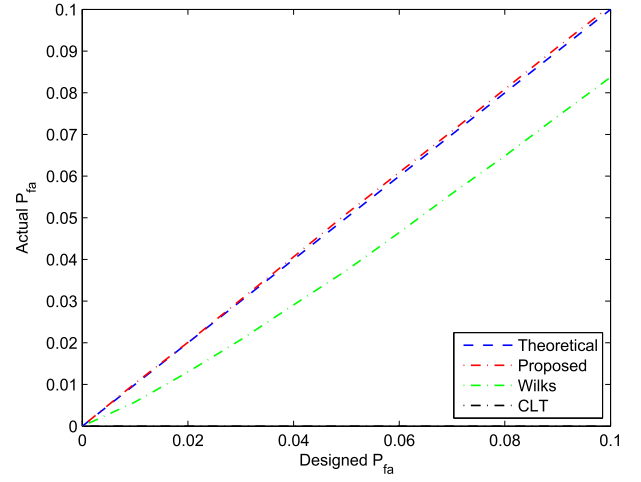
$$\mathbb{E}[\exp((it)q_0(\mathbf{X}'))q_2(\mathbf{X}')] = (it)^3 b_3 + (it)b_1 \quad (57a)$$

$$\mathbb{E}[\exp((it)q_0(\mathbf{X}'))q_1^2(\mathbf{X}')] = (it)^4 b_4 + (it)^2 b_2 + b_0. \quad (57b)$$

Here, b_k is the summation of product of the $(it)^k$ column and weight w in Tables V and VI. Substituting (50), (52), (57)



(a)



(b)

Fig. 2. Analytical threshold selection: actual P_{fa} versus designed P_{fa} . (a) $[p_1, p_2, p_3, p_4] = [1, 1, 1, 1]$, $n = 50$. (b) $[p_1, p_2, p_3] = [4, 6, 8]$, $n = 80$.

into (47), we obtain the characteristic function of T' as:

$$C'(t) = \text{etr}\left(\frac{(it)^2}{2}\mathbf{A}^2\right) \left[1 + \sum_{k=1}^6 (it)^k l_k + \mathcal{O}(n^{-\frac{3}{2}})\right], \quad (58)$$

where

$$l_1 = \frac{1}{\sqrt{n}}d_0 \quad (59a)$$

$$l_2 = \frac{1}{n}(b_0 + b_1 + d_1) \quad (59b)$$

$$l_3 = \frac{1}{\sqrt{n}}\left[d_2 + \frac{\text{tr}(\mathbf{A}^3)}{3}\right] \quad (59c)$$

$$l_4 = \frac{1}{n}\left[b_2 + b_3 + d_3 + \frac{\text{tr}(\mathbf{A}^4)}{4}\right] \quad (59d)$$

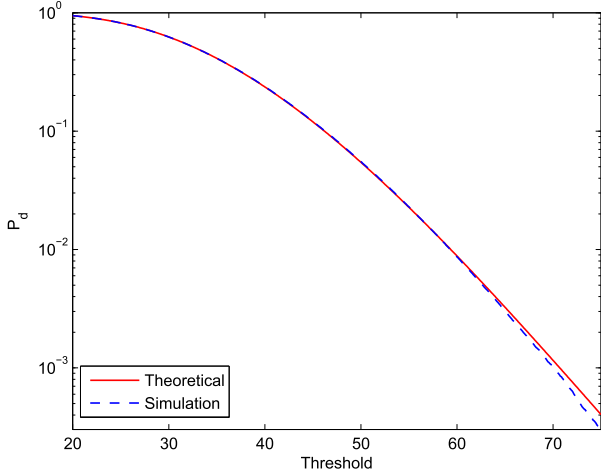
$$l_5 = 0 \quad (59e)$$

$$l_6 = \frac{1}{n}\left[b_5 + d_5 + \frac{\text{tr}^2(\mathbf{A}^3)}{18}\right]. \quad (59f)$$

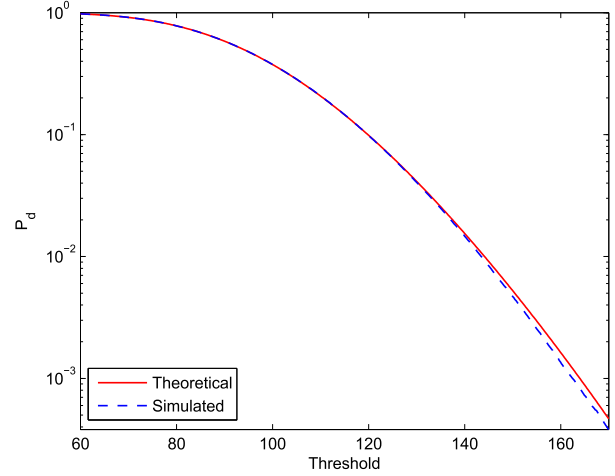
Inverting this characteristic function and using the relation $T' = (T - n\text{tr}(\mathbf{Z}^2))/\sqrt{n}$, we obtain the following theorem.

TABLE II
THRESHOLD APPROXIMATIONS FOR DIFFERENT FALSE-ALARM PROBABILITIES

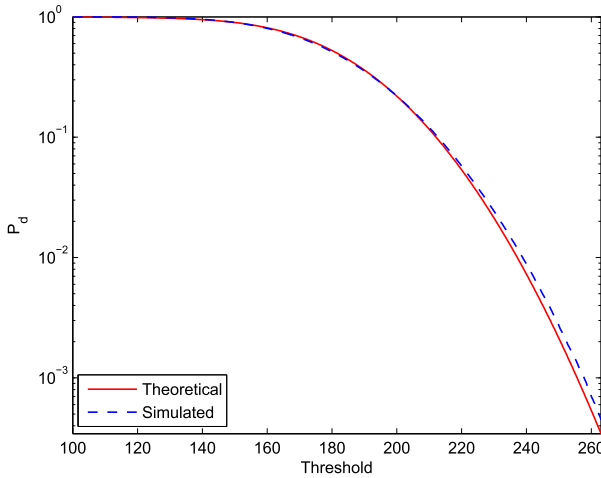
P_{fa}	$[p_1, p_2, p_3, p_4] = [1, 1, 1, 1], n = 50$				$[p_1, p_2, p_3] = [4, 6, 8], n = 80$			
	Wilks	Proposed	Simulated	CLT	Wilks	Proposed	Simulated	CLT
0.01	26.2170	25.8724	25.8900	25.1598	258.3637	254.0699	253.9152	--
0.05	21.0261	20.8066	20.8200	21.3047	242.6465	239.8666	239.7036	--



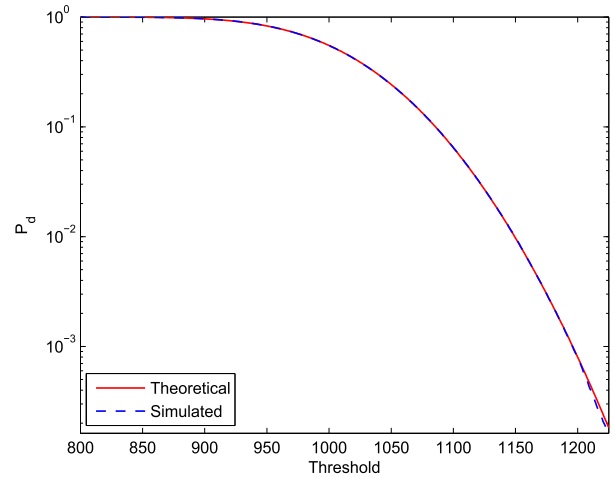
(a)



(a)



(b)



(b)

Fig. 3. Detection probability versus threshold for different SNRs, $[p_1, p_2, p_3] = [2, 3, 1], n = 100$. (a) SNR = -10dB. (b) SNR = -2dB.

Fig. 4. Detection probability versus threshold for different SNRs, $[p_1, p_2, p_3] = [2, 3, 1], n = 600$. (a) SNR = -10dB. (b) SNR = -2dB.

Theorem 3: Under far hypothesis that $(\Sigma - \mathbf{I}_p)$ is of order $\mathcal{O}(1)$, the CDF of T is approximated asymptotically up to $\mathcal{O}(n^{-\frac{3}{2}})$ by

$$\Pr(T \leq \gamma) = Q(x) + \sum_{k=1}^6 (-1)^k \frac{l_k Q^{(k)}(x)}{\tau^k} + \mathcal{O}(n^{-\frac{3}{2}}), \quad (60)$$

where $\tau = \text{tr}(\mathbf{A}^2)$, $x = \sqrt{n\tau}\gamma + n\text{tr}(\mathbf{Z}^2)$ and $Q^j(x)$ represents the j -th order derivative of the standard Gaussian CDF $Q(x)$.

It should be pointed out that τ becomes 0 as the alternative hypothesis approaches the null hypothesis. Hence, (60) is valid only when the alternative hypothesis is not close to the null hypothesis.

Remark: We have derived two asymptotic non-null distributions of the LMPIT, namely, (42) and (60) for close and far hypotheses, respectively. Recall that we pick the close hypothesis model when $(\Sigma - \mathbf{I}_p)$ is of order $\mathcal{O}(1/\sqrt{n})$ and far hypothesis model when it is of order $\mathcal{O}(1)$. Since $(\Sigma - \mathbf{I}_p)$

has $p^2 - p_2$ non-zero entries, it is reasonable to adopt (60) if $\text{tr}((\mathbf{\Sigma} - \mathbf{I})^2)/(p^2 - p_2) \gg n^{-1}$; otherwise (42) is used.

VI. NUMERICAL RESULTS

In this section, we carry out computer simulations to evaluate the accuracies of the derived asymptotic distributions for the null and alternative hypotheses, and confirm our theoretical computations for the decision threshold.

A. Null Distribution and Decision Threshold

Let us evaluate the accuracies of the false-alarm probability as well as theoretical threshold calculated by (32). For the purpose of comparison, we also present the results obtained by the Wilks' theorem in [14], that is

$$T \sim \chi_f^2, \quad (61)$$

and the result in [19] by CLT, namely

$$T \sim \mathcal{N}(f, 2p^2). \quad (62)$$

In order to quantify the approximation accuracy, we employ the Cramér-von Mises test of fit to calculate the error between the proposed and simulated CDFs, which is defined as [25]:

$$\epsilon = \frac{1}{Q} \sum_{j=1}^Q |G(x_j) - \hat{G}(x_j)|^2. \quad (63)$$

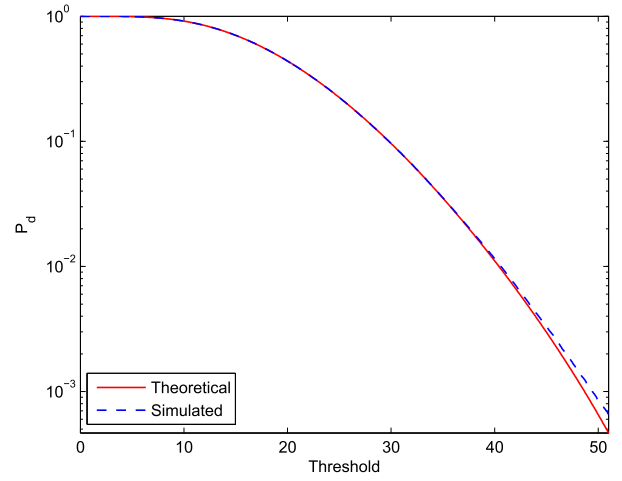
In Fig. 1, the false-alarm probability is plotted as a function of the threshold obtained from 10^6 Monte-Carlo trials with $[p_1, p_2, p_3, p_4] = [1, 1, 1, 1]$, $n = 50$ for Fig. 1(a) and $[p_1, p_2, p_3] = [4, 6, 8]$, $n = 80$ for Fig. 1(b). Note that the line of CLT is not plotted in Fig. 1(b) since the result given in [19] considers only scalar case, namely, $p_1 = \dots = p_q = 1$. It is indicated in Fig. 1 and Table I that the proposed approximation yields a much smaller error than the existing approximations derived from Wilks' theorem and CLT. The approximation of CLT leads to a relatively large error because it is inherently derived for the scenario when $p, n \rightarrow \infty$ with $p/n \rightarrow c > 0$. Thus, it is not appropriate for the small values of p . However, simulations in [19] show that this approximation is reasonably accurate when both p and n are large and comparable in size.

Fig. 2 depicts the actual P_{fa} versus designed P_{fa} , where the parameter setting remains unchanged. It is seen that the threshold (32) yields a P_{fa} which aligns very well with the theoretical one. However, the approximations using Wilks' theorem and CLT result in quite large gaps between the actual and designed false-alarm probabilities, which in turn implies that the proposed approach is much more accurate than the existing schemes.

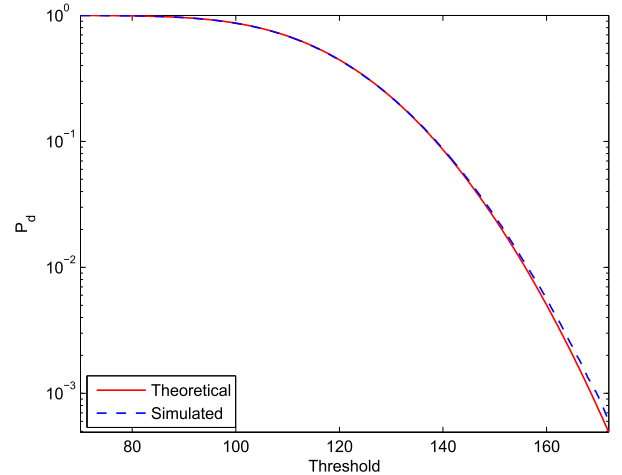
Table II provides the threshold approximations for false-alarm rates of 0.01 and 0.05. It is observed that the proposed approach is able to provide an important correction for the previous results in [14]. On the other hand, it is indicated that (32) is capable of yielding a sufficiently precise threshold.

B. Non-Null Distribution

Let us now evaluate the accuracy of the approximate non-null distributions of T , which is illustrated by the signal plus noise model. More specifically, we assume that there



(a)



(b)

Fig. 5. Detection probability versus threshold for different SNRs, $[p_1, p_2] = [2, 2]$, $n = 200$. (a) SNR = $[-9, -10]$ dB. (b) SNR = $[-1, 0]$ dB

are d independent sources with powers $\text{SNR}_1, \dots, \text{SNR}_d$. Meanwhile, the noise covariance is set to be \mathbf{I}_p without loss of generality. The channel matrix $\mathbf{H} = [\mathbf{h}_1, \dots, \mathbf{h}_d]$ has i.i.d. entries that follow standard complex Gaussian distribution and each channel vector is normalized as $\bar{\mathbf{h}}_j = \sqrt{p} \mathbf{h}_j / \|\mathbf{h}_j\|$. In the sequel, the population covariance matrix is represented as $\mathbf{\Sigma} = \mathbf{I}_p + \sum_{j=1}^d \bar{\mathbf{h}}_j \bar{\mathbf{h}}_j^H \text{SNR}_j$. In Fig. 3(a), we consider the scenario where there is $d = 1$ signal source with power of 0.1, which indicates that (42) should be applied here. Moreover, the observation dimension is $[p_1, p_2, p_3] = [2, 3, 1]$ and the number of samples is $n = 100$. It is seen that the agreement between the theoretical and simulated P_d is quite good. More precisely, the approximate error equals 4.1524×10^{-7} . In Fig. 3(b), the SNR is changed to -2 dB. Accordingly, (60) is used here. The error between the approximate and simulated detection probabilities is 1.2430×10^{-5} . In Fig. 4, we modify n to be 600, but keep other parameters unchanged. It is observed that the agreement between the simulated and analytical results is better than that in the case of $n = 100$,

and the approximation error reduces to 2.6571×10^{-7} and 2.5546×10^{-7} at SNR = -10 dB and SNR = -2 dB, respectively. This indicates the errors decrease as the number of samples increases.

Another parameter setting is used in Fig. 5, that is, $d = 2$, $[p_1, p_2] = [2, 2]$, $n = 200$ and SNR equals $[-9, -10]$ dB in Fig. 5(a) and $[-1, 0]$ dB in Fig. 5(b). The errors between the approximate and simulated detection probabilities are 8.8111×10^{-8} and 1.3338×10^{-6} for the low and high SNR cases, respectively. This confirms that the analytical calculations are very accurate for both single- and multiple-source cases.

VII. CONCLUSION

In this paper, we have derived the asymptotic formulae for the distributions of the LMPIT by inverting the asymptotic series expansion of its characteristic function. Under the null hypothesis, the result is expressed as a function of Chi-squared CDFs, ending up with a simple and accurate expression for threshold calculation. Besides, the non-null distributions are derived for the close hypothesis in terms of non-central Chi-squared CDFs, whereas for the far hypothesis in terms of weighted sum of Gaussian CDF and its derivatives. The convergence rates are $\mathcal{O}(n^{-2})$ and $\mathcal{O}(n^{-\frac{3}{2}})$ for the null and alternative hypotheses, respectively. Extensive simulation results demonstrate the accuracies of the derived asymptotic distributions.

APPENDIX A ASYMPTOTIC DISTRIBUTION OF \mathbf{Y}

In the real-valued situation, the Jacobian transformation of \mathbf{S} to \mathbf{Y} is obtained from [26] (See Lemma 8), which can be generalized to the complex-valued case.

Let $\mathbf{Y} = \mathbf{U}^H \mathbf{\Lambda} \mathbf{U}$ and $\mathbf{S} = \mathbf{U}^H \mathbf{\Lambda}' \mathbf{U}$ be the eigenvalue decompositions (EVDs) of \mathbf{Y} and \mathbf{S} , respectively. Here, $\mathbf{\Lambda} = \text{diag}(\lambda_1, \dots, \lambda_p)$ and $\mathbf{\Lambda}' = \text{diag}(f(\lambda_1), \dots, f(\lambda_p))$ with $f(x) = ne^{\frac{x}{\sqrt{n}}}$. Then the Jacobian transformation between \mathbf{S} and \mathbf{Y} is expressed as

$$\left| \frac{\partial \mathbf{S}}{\partial \mathbf{Y}} \right| = \left| \frac{\partial \mathbf{S}}{\partial (\mathbf{U}, \mathbf{\Lambda}')} \cdot \frac{\partial (\mathbf{U}, \mathbf{\Lambda}')}{\partial (\mathbf{U}, \mathbf{\Lambda})} \cdot \frac{\partial (\mathbf{U}, \mathbf{\Lambda})}{\partial \mathbf{Y}} \right|. \quad (64)$$

Note that the second term is easily calculated as

$$\left| \frac{\partial (\mathbf{U}, \mathbf{\Lambda}')}{\partial (\mathbf{U}, \mathbf{\Lambda})} \right| = \left| \frac{\partial (\mathbf{\Lambda}')}{\partial (\mathbf{\Lambda})} \right| = \prod_{i=1}^p f'(\lambda_i) = n^{\frac{p}{2}} \text{etr} \left(\frac{\mathbf{Y}}{\sqrt{n}} \right). \quad (65)$$

On the other hand, we have

$$\begin{aligned} \mathbf{J}_p &\triangleq \left| \frac{\partial \mathbf{Y}}{\partial (\mathbf{U}, \mathbf{\Lambda})} \right| = \left| \frac{\partial (\mathbf{U}_0' \mathbf{Y} \mathbf{U}_0)}{\partial (\mathbf{U}, \mathbf{\Lambda})} \right| = \left| \frac{\partial \mathbf{G}}{\partial \mathbf{U}} \right| \left| \frac{\partial (\mathbf{U}_0' \mathbf{Y} \mathbf{U}_0)}{\partial (\mathbf{\Lambda}, \mathbf{G})} \right| \\ &= \left| \frac{\partial \mathbf{G}}{\partial \mathbf{U}} \right| \left| \frac{\partial \mathbf{Y}^*}{\partial (\mathbf{U}, \mathbf{G})} \right| = \left| \frac{\partial \mathbf{G}}{\partial \mathbf{U}} \right| \mathbf{J}_p^*. \end{aligned} \quad (66)$$

where \mathbf{U}_0 is an orthogonal matrix such that $\mathbf{U}_0 \mathbf{U}$ is approximately equal to the identity matrix, namely, $\mathbf{U}_0 \mathbf{U} = \mathbf{I}_p + \mathbf{G}$

and $\mathbf{U} \mathbf{U}_0 = \mathbf{I}_p - \mathbf{G}$. Then, we obtain

$$\begin{aligned} \mathbf{Y}^* &= \begin{bmatrix} \mathbf{Y}_{p-1}^* & \boldsymbol{\xi} \\ \boldsymbol{\xi} & y \end{bmatrix} \\ &= \mathbf{\Lambda} + \mathbf{\Lambda} \mathbf{G} - \mathbf{G} \mathbf{\Lambda} - \mathbf{G}^2 \\ &= \begin{bmatrix} \mathbf{\Lambda}_{p-1} & \mathbf{0} \\ \mathbf{0} & \lambda_p \end{bmatrix} + \begin{bmatrix} \mathbf{G}_{p-1} & \boldsymbol{\tau} \\ -\boldsymbol{\tau}' & 0 \end{bmatrix} \begin{bmatrix} \mathbf{\Lambda}_{p-1} & \mathbf{0} \\ \mathbf{0} & \lambda_p \end{bmatrix} \\ &\quad - \begin{bmatrix} \mathbf{\Lambda}_{p-1} & \mathbf{0} \\ \mathbf{0} & \lambda_p \end{bmatrix} - \mathbf{G}^2 \\ &= \begin{bmatrix} \mathbf{\Lambda}_{p-1} + \mathbf{\Lambda}_{p-1} \mathbf{G}_{p-1} - \mathbf{G}_{p-1} \mathbf{\Lambda}_{p-1} & \mathbf{\Lambda}_{p-1} \boldsymbol{\tau} - \lambda_p \boldsymbol{\tau} \\ -\boldsymbol{\tau}' \mathbf{\Lambda}_{p-1} - \lambda_p \boldsymbol{\tau}' & \lambda_p \end{bmatrix} - \mathbf{G}^2. \end{aligned} \quad (67)$$

It follows that

$$\begin{aligned} \mathbf{J}_p^* &= \left| \frac{\partial (\mathbf{Y}_{p-1}, \boldsymbol{\xi}, y)}{\partial (\mathbf{\Lambda}_{p-1}, \mathbf{G}_{p-1}, \boldsymbol{\tau}, \lambda_p)} \right| \\ &= \mathbf{J}_{p-1}^* \left| \frac{\partial (\boldsymbol{\xi}, y)}{\partial (\boldsymbol{\xi}, \lambda_p)} \right| \left| \frac{\partial (\boldsymbol{\xi}, \lambda_p)}{\partial (\boldsymbol{\tau}, \lambda_p)} \right| \\ &= \left| \frac{\partial \boldsymbol{\xi}}{\partial \boldsymbol{\tau}} \right| \left| \frac{\partial y}{\partial \lambda_p} \right| \mathbf{J}_{p-1}^* \\ &= |\mathbf{\Lambda}_{p-1} - \lambda_p \mathbf{I}_{p-1}|^2 \mathbf{J}_{p-1}^* \\ &= \mathbf{J}_{p-1}^* \prod_{i=1}^{p-1} (\lambda_p - \lambda_i)^2 \\ &= \prod_{i>j} (\lambda_i - \lambda_j)^2. \end{aligned} \quad (68)$$

Therefore, we have

$$\left| \frac{\partial \mathbf{S}}{\partial (\mathbf{U}, \mathbf{\Lambda}')} \cdot \frac{\partial (\mathbf{U}, \mathbf{\Lambda}')}{\partial \mathbf{Y}} \right| = \left[\prod_{i>j}^p \frac{f(\lambda_i) - f(\lambda_j)}{\lambda_i - \lambda_j} \right]^2. \quad (69)$$

Substituting (69) and (65) into (64), the Jacobian transformation of \mathbf{S} to \mathbf{Y} is

$$\left| \frac{\partial \mathbf{S}}{\partial \mathbf{Y}} \right| = n^{\frac{p^2}{2}} \text{etr} \left(\frac{\mathbf{Y}}{\sqrt{n}} \right) \prod_{i>j}^p \left[\frac{\exp(\frac{1}{\sqrt{n}} \lambda_i) - \exp(\frac{1}{\sqrt{n}} \lambda_j)}{\frac{1}{\sqrt{n}} \lambda_i - \frac{1}{\sqrt{n}} \lambda_j} \right]^2. \quad (70)$$

Moreover, the last term on the RHS of (70) can be further expanded for large n , that is,

$$\begin{aligned} &\prod_{i>j}^p \left[\frac{\exp(\frac{1}{\sqrt{n}} \lambda_i) - \exp(\frac{1}{\sqrt{n}} \lambda_j)}{\frac{1}{\sqrt{n}} \lambda_i - \frac{1}{\sqrt{n}} \lambda_j} \right]^2 \\ &= 1 + \frac{p-1}{\sqrt{n}} \text{tr}(\mathbf{Y}) + \frac{6p^2 - 12p + 5}{12n} \text{tr}^2(\mathbf{Y}) + \frac{p}{12n} \text{tr}(\mathbf{Y}^2) + \mathcal{O}(n^{-\frac{3}{2}}). \end{aligned} \quad (71)$$

Since \mathbf{Y} is a square matrix, we have $|\mathbf{e}^{\mathbf{Y}}| = \text{etr}(\mathbf{Y})$. It follows that the asymptotic distribution of \mathbf{Y} is given by

$$\begin{aligned} f_{\mathbf{Y}}(\mathbf{Y} | \mathcal{H}_0) &= c \cdot \text{etr} \left(\frac{n-p+1}{\sqrt{n}} \mathbf{Y} - ne^{\frac{1}{\sqrt{n}} \mathbf{Y}} \right) \left[1 + \frac{p-1}{\sqrt{n}} \text{tr}(\mathbf{Y}) \right. \\ &\quad \left. + \frac{6p^2 - 12p + 5}{12n} \text{tr}^2(\mathbf{Y}) + \frac{p}{12n} \text{tr}(\mathbf{Y}^2) + \mathcal{O}(n^{-\frac{3}{2}}) \right], \end{aligned} \quad (72)$$

where $c = N^{p(N-\frac{p}{2})} \pi^{-\frac{p(p-1)}{2}} [\prod_{k=1}^p (\Gamma(n+1-k))]^{-1}$. and Notice that

$$e^{\frac{1}{\sqrt{n}}\mathbf{Y}} = \mathbf{I}_p + \frac{\mathbf{Y}}{\sqrt{n}} + \frac{\mathbf{Y}^2}{2n} + \frac{\mathbf{Y}^3}{6\sqrt{n}^3} + \frac{\mathbf{Y}^4}{24n^2} + \mathcal{O}(n^{-\frac{5}{2}}), \quad (73)$$

which, when substituted into (72), leads to

$$f_{\mathbf{Y}}(\mathbf{Y}|\mathcal{H}_0) = c_1 \cdot \text{etr} \left(-\frac{\mathbf{Y}^2}{2} \right) \left[1 - \frac{\text{tr}(\mathbf{Y}^3)}{6\sqrt{n}} - \frac{\text{tr}^2(\mathbf{Y})}{12n} + \frac{p\text{tr}(\mathbf{Y}^2)}{12n} - \frac{\text{tr}(\mathbf{Y}^4)}{24n} + \frac{\text{tr}^2(\mathbf{Y}^3)}{72n} + \mathcal{O}(n^{-\frac{3}{2}}) \right], \quad (74)$$

where $c_1 = c \times \exp(-np)$.

APPENDIX B ASYMPTOTIC SERIES EXPANSION OF T

The asymptotic series expansion of \mathbf{S} is easily calculated as

$$\frac{\mathbf{S}}{n} = \mathbf{I}_p + \frac{\mathbf{Y}}{\sqrt{n}} + \frac{\mathbf{Y}^2}{2n} + \frac{\mathbf{Y}^3}{6\sqrt{n}^3} + \frac{\mathbf{Y}^4}{24n^2} + \mathcal{O}(n^{-\frac{5}{2}}). \quad (75)$$

To determine the expansion of \mathbf{S}_D^{-1} , we need the result from [27, p. 55], which is presented as follows.

Lemma 2: Let $\mathbf{A} \in \mathbb{C}^{p \times p}$ and $\lim_{k \rightarrow \infty} \mathbf{A}^k = \mathbf{0}_{p \times p}$. Then $\mathbf{I}_p - \mathbf{A}$ is nonsingular and

$$(\mathbf{I}_p - \mathbf{A})^{-1} = \sum_{k=0}^{\infty} \mathbf{A}^k. \quad (76)$$

As a result, we can expand \mathbf{S}_D^{-1} as

$$\begin{aligned} \left(\frac{\mathbf{S}_D}{n} \right)^{-1} &= \left(\mathbf{I}_p + \frac{\mathbf{Y}_D}{\sqrt{n}} + \frac{(\mathbf{Y}^2)_D}{2n} + \frac{(\mathbf{Y}^3)_D}{6\sqrt{n}^3} \right. \\ &\quad \left. + \frac{(\mathbf{Y}^4)_D}{24n^2} + \mathcal{O}(n^{-\frac{5}{2}}) \right)^{-1} \\ &= \mathbf{I}_p - \frac{1}{\sqrt{n}}\mathbf{Y}_D + \frac{1}{n} \left[-\frac{1}{2}(\mathbf{Y}^2)_D + \mathbf{Y}_D^2 \right] \\ &\quad + \frac{1}{\sqrt{n}^3} \left[-\frac{1}{6}(\mathbf{Y}^3)_D + \mathbf{Y}_D(\mathbf{Y}^2)_D - \mathbf{Y}_D^3 \right] \\ &\quad + \frac{1}{n^2} \left[\frac{1}{3}(\mathbf{Y}^3)_D\mathbf{Y}_D + \frac{1}{4}(\mathbf{Y}^2)_D^2 - \frac{1}{24}(\mathbf{Y}^4)_D \right. \\ &\quad \left. - \frac{3}{2}\mathbf{Y}_D^2(\mathbf{Y}^2)_D + \mathbf{Y}_D^4 \right] + \mathcal{O}(n^{-\frac{5}{2}}). \quad (77) \end{aligned}$$

Substituting (75) and (77) into (10) leads to the asymptotic series expansion of T :

$$\begin{aligned} T &= \text{tr}(\mathbf{Y}^2 - \mathbf{Y}_D^2) + \frac{1}{\sqrt{n}}\text{tr} \left[2\mathbf{Y}_D^3 - 3\mathbf{Y}^2\mathbf{Y}_D + \mathbf{Y}^3 \right] \\ &\quad + \frac{1}{n}\text{tr} \left[\frac{7}{12}\mathbf{Y}^4 + 5\mathbf{Y}^2\mathbf{Y}_D^2 - \frac{7}{3}\mathbf{Y}_D\mathbf{Y}^3 + (\mathbf{Y}\mathbf{Y}_D)^2 \right. \\ &\quad \left. - \frac{5}{4}(\mathbf{Y}^2)_D^2 - 3\mathbf{Y}_D^4 \right] + \mathcal{O}(n^{-\frac{3}{2}}). \quad (78) \end{aligned}$$

Alternatively, when using $\mathbf{X} = (\mathbf{S} - n\boldsymbol{\Sigma})/\sqrt{n}$, it is straightforward to obtain

$$\mathbf{S} = \sqrt{n}\mathbf{X} + n\boldsymbol{\Sigma} \quad (79)$$

$$\begin{aligned} \left(\frac{\mathbf{S}_D}{n} \right)^{-1} &= \mathbf{I}_p - \frac{1}{\sqrt{n}}\mathbf{X}_D + \frac{1}{n}(\mathbf{X}_D)^2 - \frac{1}{\sqrt{n}^3}(\mathbf{X}_D)^3 \\ &\quad + \frac{1}{n^2}(\mathbf{X}_D)^4 + \mathcal{O}(n^{-\frac{5}{2}}). \quad (80) \end{aligned}$$

Combining (79) and (80) together, we eventually have

$$\begin{aligned} T &= n\text{tr}(\mathbf{Z}'^2) + \sqrt{n}\text{tr}[2\mathbf{Z}'(\mathbf{X} - \boldsymbol{\Sigma}\mathbf{X}_D)] \\ &\quad + \text{tr}[2\mathbf{Z}'(\boldsymbol{\Sigma}(\mathbf{X}_D)^2 - \mathbf{X}\mathbf{X}_D) + (\mathbf{X} - \boldsymbol{\Sigma}\mathbf{X}_D)^2] \\ &\quad + \frac{1}{\sqrt{n}}\text{tr}[2\mathbf{Z}'(-\boldsymbol{\Sigma}(\mathbf{X}_D)^3 + \mathbf{X}(\mathbf{X}_D)^2) \\ &\quad + 2(\mathbf{X} - \boldsymbol{\Sigma}\mathbf{X}_D)(\boldsymbol{\Sigma}(\mathbf{X}_D)^2 - \mathbf{X}\mathbf{X}_D)] + \mathcal{O}(n^{-1}). \quad (81) \end{aligned}$$

APPENDIX C DERIVATION OF MOMENTS IN (22) AND (39)

In this appendix we present the moments involved in (22) and (39), as well as typical examples of their derivations.

According to (19), the expectation of $\text{tr}(\mathbf{Y}'^4)$ in (22) is,

$$\begin{aligned} \mathbb{E}[\text{tr}(\mathbf{Y}'^4)] &= \mathbb{E} \left[2 \sum_{\substack{j,k,l=1 \\ j \neq k \neq l}}^p \mathbf{Y}'_{j,k} \mathbf{Y}'_{k,j} \mathbf{Y}'_{j,l} \mathbf{Y}'_{l,j} + \sum_{\substack{j,k=1 \\ j \neq k}}^p \mathbf{Y}'_{j,k}^2 \mathbf{Y}'_{k,j}^2 \right. \\ &\quad \left. + 4 \sum_{\substack{j,k=1 \\ j \neq k}}^p \mathbf{Y}'_{j,j}^2 \mathbf{Y}'_{j,k} \mathbf{Y}'_{k,j} + \sum_{j=1}^p \mathbf{Y}'_{j,j}^4 \right] \\ &= 2[(p_3 + p_2 - 2pp_2 + p^3 - p^2)\phi^2 \\ &\quad + 2(-p_3 + pp_2 + p_2 - p^2)\phi + p_3 - 3p_2 + 2p] \\ &\quad + [2(p^2 - p_2)\phi^2 + 2p_2 - 2p] \\ &\quad + 4[(p^2 - p_2)\phi + p_2 - p] + 3p \\ &= (2p^3 + 2\tilde{p}_3 - 4p\tilde{p}_2)\phi^2 + (4p\tilde{p}_2 - 4\tilde{p}_3)\phi + 2\tilde{p}_3 + p. \quad (82) \end{aligned}$$

Similarly, the other moments in (22) are also calculated, which are tabulated in Table III.

In (39), the random matrix \mathbf{Y}'' is further influenced by an additive term $\phi\mathbf{Z}$. Therefore, the expectations should be calculated in a slightly different manner. Here we take $\text{tr}(\mathbf{Y}''^4)$ as an example. The detailed calculations of the remaining components are omitted due to the space limit, but their expressions are given in Table IV. The mathematical expectation of $\text{tr}(\mathbf{Y}''^4)$ is

$$\begin{aligned} \mathbb{E}[\text{tr}(\mathbf{Y}''^4)] &= 2 \sum_{\substack{j,k,l=1 \\ j \neq k \neq l}}^p (|\mathbf{Z}_{j,k}|^2\phi^2 + \sigma_{j,k}^2)(|\mathbf{Z}_{l,k}|^2\phi^2 + \sigma_{l,k}^2) \\ &\quad + \sum_{\substack{j,k=1 \\ j \neq k}}^p (|\mathbf{Z}_{j,k}|^4\phi^4 + 4|\mathbf{Z}_{j,k}|^2\sigma_{j,k}^2\phi^2 + 2\sigma_{j,k}^4) \\ &\quad + 4 \sum_{\substack{j,k=1 \\ j \neq k}}^p (|\mathbf{Z}_{j,k}|^2\phi^2 + \sigma_{j,k}^2) + \sum_{j=1}^p 3 \\ &= a_4\phi^4 + (4pa_2 - 4c)\phi^3 + (2\tilde{p}_3 - 4p\tilde{p}_2 + 2p^3 + 4c)\phi^2 \\ &\quad + (4p\tilde{p}_2 - 4\tilde{p}_3)\phi + 2\tilde{p}_3 + p, \quad (83) \end{aligned}$$

where $\sigma_{j,k}^2 = 2v_{j,k}$.

TABLE III
EXPECTED VALUES INVOLVED IN (22)

	Expected value
$\text{tr}^2(\mathbf{Y}')$	p
$\text{tr}(\mathbf{Y}'^2)$	$(p^2 - \bar{p}_2)\phi + \bar{p}_2$
$\text{tr}(\mathbf{Y}'_D^4)$	$2\bar{p}_3 + p$
$\text{tr}(\mathbf{Y}'^4)$	$(2p^3 + 2\bar{p}_3 - 4p\bar{p}_2)\phi^2 + (4p\bar{p}_2 - 4\bar{p}_3)\phi + 2\bar{p}_3 + p$
$\text{tr}(\mathbf{Y}'^3 \mathbf{Y}'_D)$	$(2p\bar{p}_2 - 2\bar{p}_3)\phi + 2\bar{p}_3 + p$
$\text{tr}(\mathbf{Y}'^2 \mathbf{Y}'_D^2)$	$(p\bar{p}_2 - p^3)\phi + 2\bar{p}_3 + p$
$\text{tr}((\mathbf{Y}' \mathbf{Y}'_D)^2)$	$2\bar{p}_3 + p$
$\text{tr}((\mathbf{Y}'^2)_D^2)$	$(p^3 - p\bar{p}_2)\phi^2 + (2p\bar{p}_2 - 2\bar{p}_3)\phi + 2\bar{p}_3 + p$
$\text{tr}^2(\mathbf{Y}'^3)$	$(3p^3 + 6\bar{p}_3 - 9p\bar{p}_2)\phi^3 + (9p^3 - 9p\bar{p}_2)\phi^2 + (18p\bar{p}_2 - 18\bar{p}_3)\phi + 12\bar{p}_3 + 3p$
$\text{tr}^2(\mathbf{Y}'_D^3)$	$12\bar{p}_3 + 3p$
$\text{tr}^2(\mathbf{Y}'^2 \mathbf{Y}'_D)$	$(p^3 - p\bar{p}_2)\phi^2 + (6p\bar{p}_2 - 6\bar{p}_3)\phi + 12\bar{p}_3 + 3p$
$\text{tr}(\mathbf{Y}'^3) \text{tr}(\mathbf{Y}'_D^3)$	$(9p\bar{p}_2 - 9\bar{p}_3)\phi + 12\bar{p}_3 + 3p$
$\text{tr}(\mathbf{Y}'^3) \text{tr}(\mathbf{Y}'^2 \mathbf{Y}'_D)$	$(3p^3 - 3p\bar{p}_2 + 12c)\phi^2 + (12p\bar{p}_2 - 12\bar{p}_3)\phi + 12\bar{p}_3 + 3p$
$\text{tr}(\mathbf{Y}'^2 \mathbf{Y}'_D) \text{tr}(\mathbf{Y}'_D^3)$	$(3p\bar{p}_2 - 3\bar{p}_3)\phi + 12\bar{p}_3 + 3p$

APPENDIX D
STIRLING'S APPROXIMATION OF c_2

In this appendix, we calculate Stirling's approximation of the constant c_2 , which is expressed as

$$c_2 = (2\pi)^{\frac{p}{2}} n^{(n-\frac{p}{2})p} \exp(-pn) \left[\prod_{k=1}^p \Gamma(n+1-k) \right]^{-1} \\ = \prod_{k=1}^p \left[\sqrt{2\pi} \frac{n^{(n-k+\frac{1}{2})}}{\Gamma(n+1-k)} \exp(-n) \right]. \quad (84)$$

It follows from [28] that the Stirling's formula is

$$\frac{(n-k)^{n-k+\frac{1}{2}} \sqrt{2\pi}}{e^{n-k} \Gamma(n+1-k)} = 1 - \frac{1}{12(n-k)} + \mathcal{O}(n^{-2}). \quad (85)$$

With the use of (85), each product term in (84) is

$$\frac{\sqrt{2\pi} n^{(n-k+\frac{1}{2})} e^{-n}}{\Gamma(n+1-k)} = e^{-k} \left(\frac{n}{n-k} \right)^{n-k+\frac{1}{2}} \\ \times \left[1 - \frac{1}{12(n-k)} + \mathcal{O}(n^{-2}) \right]. \quad (86)$$

Note that

$$\left(\frac{n}{n-k} \right)^{n-k+\frac{1}{2}} = e^{\frac{k}{n-k}(n-k+\frac{1}{2})} - \frac{k^2}{2n} e^k + \mathcal{O}(n^{-2}). \quad (87)$$

which, when substituted into (86), yields

$$\frac{\sqrt{2\pi} n^{(n-\frac{k}{2})} e^{-n}}{\Gamma(n+1-k)} = \left[e^{\frac{k}{2(n-k)}} - \frac{k^2}{2n} + \mathcal{O}(n^{-2}) \right] \\ \times \left[1 - \frac{1}{12(n-k)} + \mathcal{O}(n^{-2}) \right]. \quad (88)$$

Consequently, the Stirling's approximation for c_2 is

$$c_2 = \prod_{k=1}^p \left\{ \left[e^{\frac{k}{2(n-k)}} - \frac{k^2}{2n} + \mathcal{O}(n^{-2}) \right] \right. \\ \times \left. \left[1 - \frac{1}{12(n-k)} + \mathcal{O}(n^{-2}) \right] \right\} \\ = \left[1 - \frac{2p^3 - 2p}{12n} + \mathcal{O}(n^{-2}) \right] \left[1 - \frac{p}{12n} + \mathcal{O}(n^{-2}) \right] \\ = 1 - \frac{2p^3 - p}{12n} + \mathcal{O}(n^{-2}). \quad (89)$$

APPENDIX E
DERIVATION OF MOMENTS IN (52) AND (55)

For illustrative purposes, we first consider the term $\text{tr}(\mathbf{S}^2)$:

$$\mathbb{E}[\exp((it)q_0(\mathbf{X})) \text{tr}(\mathbf{S}^2)] \\ = \mathbb{E}[\exp((it)q_0(\mathbf{X})) \sum_{i,j=1}^p (\mathbf{S}_{i,j} \mathbf{S}_{j,i})] \\ = |\Psi \Sigma^{-1}|^n (n^2 \sum_{i,j=1}^p (\Psi_{i,j} \Psi_{j,i}) + n \Psi_{i,i} \Psi_{j,j}) \\ = |\Psi \Sigma^{-1}|^n (n^2 \text{tr}(\Psi^2) + n \text{tr}^2(\Psi)). \quad (90)$$

Using similar manipulations, the mathematical expectations of the subsequent terms are readily obtained, which, when summed up, leads to

$$\mathbb{E}[q_1(\mathbf{X}) \exp((it)q_0(\mathbf{X}))] \\ = |\Psi \Sigma^{-1}|^n \left\{ n^2 [\text{tr}(\Psi^2) + \text{tr}(\Sigma \Psi_D \Psi) + \text{tr}(\Sigma \Psi_D \Sigma \Psi) \\ + \text{tr}(\mathbf{Z}' \Psi \Psi_D) + \text{tr}(\mathbf{Z}' \Sigma \Psi_D^2)] + n [\text{tr}^2(\Psi) + \text{tr}^2(\Sigma \mathbf{G} \Psi) \\ + \sum_{x,y=1}^q \text{tr}^2(\Sigma_{xy} \Psi_{yx}) + \text{tr}(\mathbf{Z}' \Psi \mathbf{G}) + \text{tr}(\mathbf{Z}' \Sigma \mathbf{G} \Psi_D) \\ + \text{tr}(\mathbf{Z}' \Psi) + \text{tr}(\mathbf{Z}' \Sigma \Psi_D)] \right\}, \quad (91)$$

TABLE IV
EXPECTED VALUES INVOLVED IN (39)

	Expected value
$\text{tr}^2(\mathbf{Y}'')$	p
$\text{tr}(\mathbf{Y}''^2)$	$a_2\phi^2 + (p^2 - \tilde{p}_2)\phi + \tilde{p}_2$
$\text{tr}(\mathbf{Y}''^3_D)$	0
$\text{tr}(\mathbf{Y}''^3)$	$a_3\phi^3$
$\text{tr}(\mathbf{Y}''^2\mathbf{Z})$	$a_3\phi^2$
$\text{tr}(\mathbf{Y}''\mathbf{Z}^2)$	$a_3\phi$
$\text{tr}(\mathbf{Y}''^4_D)$	$2\tilde{p}_3 + p$
$\text{tr}(\mathbf{Y}''^4)$	$a_4\phi^4 + (4pa_2 - 4c)\phi^3 + (2\tilde{p}_3 - 4p\tilde{p}_2 + 2p^3 + 4c)\phi^2 + (4p\tilde{p}_2 - 4\tilde{p}_3)\phi + (2\tilde{p}_3 + p)$
$\text{tr}(\mathbf{Y}''^3\mathbf{Z})$	$a_4\phi^3 + (2pa_2 - 2c)\phi^2 + 2c\phi$
$\text{tr}(\mathbf{Y}''\mathbf{Z}^3)$	$a_4\phi$
$\text{tr}(\mathbf{Y}''^2\mathbf{Z}^2)$	$a_4\phi^2 + (pa_2 - c)\phi + c$
$\text{tr}(\mathbf{Y}''^2\mathbf{Y}''_D)$	0
$\text{tr}(\mathbf{Y}''^3\mathbf{Y}''_D)$	$2c\phi^2 + (2p\tilde{p}_2 - 2\tilde{p}_3)\phi + 2\tilde{p}_3 + p$
$\text{tr}(\mathbf{Y}''^2\mathbf{Y}''_D^2)$	$c\phi^2 + (p\tilde{p}_2 - p3)\phi + 2\tilde{p}_3 + p$
$\text{tr}((\mathbf{Y}''\mathbf{Y}''_D)^2)$	$2\tilde{p}_3 + p$
$\text{tr}((\mathbf{Y}''^2_D)^2)$	$b\phi^4 + 2pa_2\phi^3 + (p^3 - p\tilde{p}_2 + 2c)\phi^2 + (2p\tilde{p}_2 - 2\tilde{p}_3)\phi + 2\tilde{p}_3 + p$
$\text{tr}^2(\mathbf{Y}''^3)$	$a_3^2\phi^6 + (9a_4 - 9b)\phi^5 + (9pa_2 + 9b - 18c)\phi^4 + (3p^3 + 6\tilde{p}_3 - 9p\tilde{p}_2 + 18pa_2)\phi^3$ $+ (9p^3 + 18c - 9p\tilde{p}_2)\phi^2 + (18p\tilde{p}_2 - 18\tilde{p}_3)\phi + 12\tilde{p}_3 + 3p$
$\text{tr}^2(\mathbf{Y}''^3_D)$	$12\tilde{p}_3 + 3p$
$\text{tr}^2(\mathbf{Y}''\mathbf{Z}^2)$	$a_3^2\phi^2 + (a_4 - b)\phi + b$
$\text{tr}^2(\mathbf{Y}''^2\mathbf{Z})$	$a_3^2\phi^4 + (4a_4 - 4b)\phi^3 + (pa_2 + 4b - 2c)\phi^2 + 2c\phi$
$\text{tr}^2(\mathbf{Y}''^2\mathbf{Y}''_D)$	$b\phi^4 + 2pa_2\phi^3 + (p^3 - p\tilde{p}_2 + 6c)\phi^2 + (6p\tilde{p}_2 - 6\tilde{p}_3)\phi + 12\tilde{p}_3 + 3p$
$\text{tr}(\mathbf{Y}''^3)\text{tr}(\mathbf{Y}''^3_D)$	$9c\phi^2 + (9p\tilde{p}_2 - 9\tilde{p}_3)\phi + 12\tilde{p}_3 + 3p$
$\text{tr}(\mathbf{Y}''^2\mathbf{Z})\text{tr}(\mathbf{Y}''^3_D)$	$6c\phi$
$\text{tr}(\mathbf{Y}''\mathbf{Z}^2)\text{tr}(\mathbf{Y}''^3_D)$	$3c$
$\text{tr}(\mathbf{Y}''^3)\text{tr}(\mathbf{Y}''^2\mathbf{Y}''_D)$	$3b\phi^4 + 6pa_2\phi^3 + (3p^3 - 3p\tilde{p}_2 + 12c)\phi^2 + (12p\tilde{p}_2 - 12\tilde{p}_3)\phi + 12\tilde{p}_3 + 3p$
$\text{tr}(\mathbf{Y}''^2\mathbf{Z})\text{tr}(\mathbf{Y}''^3)$	$a_3^2\phi^5 + (6a_4 - 6b)\phi^4 + (3pa_2 + 6b - 6c)\phi^3 + 6pa_2\phi^2 + 6c\phi$
$\text{tr}(\mathbf{Y}''\mathbf{Z}^2)\text{tr}(\mathbf{Y}''^3)$	$a_3^2\phi^4 + (3a_4 - 3b)\phi^3 + 3b\phi^2 + (3pa_2 - 3c)\phi + 3c$
$\text{tr}(\mathbf{Y}''^2\mathbf{Y}''_D)\text{tr}(\mathbf{Y}''^3_D)$	$3c\phi^2 + (3p\tilde{p}_2 - 3\tilde{p}_3)\phi + 12\tilde{p}_3 + 3p$
$\text{tr}(\mathbf{Y}''\mathbf{Z}^2)\text{tr}(\mathbf{Y}''^2\mathbf{Z})$	$a_3^2\phi^3 + (2a_4 - 2b)\phi^2 + 2b\phi$
$\text{tr}(\mathbf{Y}''\mathbf{Z}^2)\text{tr}(\mathbf{Y}''^2\mathbf{Y}''_D)$	$b\phi^2 + (pa_2 - c)\phi + 3c$
$\text{tr}(\mathbf{Y}''^2\mathbf{Z})\text{tr}(\mathbf{Y}''^2\mathbf{Y}''_D)$	$2b\phi^3 + 2pa_2\phi^2 + 6c\phi$

TABLE V
EXPECTED VALUES INVOLVED IN $\mathbb{E}[q_2(\mathbf{X}')]]$

	w	$(it)^3$	it
$\text{tr}(\mathbf{Z}'\Sigma\mathbf{X}'^3_D)$	-2	$\text{tr}(\mathbf{Z}'\Sigma\mathbf{V}_D^3)$	$2\text{tr}(\mathbf{V}_D(\mathbf{Z}'\Sigma)_D\mathbf{G}_1) + \text{tr}(\mathbf{V}_D\mathbf{G}_3)$
$\text{tr}(\mathbf{Z}'\mathbf{X}'\mathbf{X}'^2_D)$	2	$\text{tr}(\mathbf{Z}'\mathbf{V}\mathbf{V}_D^2)$	$\text{tr}((\mathbf{Z}'\Sigma)_D\mathbf{V}_D\mathbf{G}_1) + \text{tr}((\mathbf{Z}'\mathbf{V})_D\mathbf{G}_1) + \text{tr}(\mathbf{V}_D\mathbf{G}_4)$
$\text{tr}(\mathbf{X}'^2\mathbf{X}'_D)$	-2	$\text{tr}(\mathbf{V}^2\mathbf{V}_D)$	$p\text{tr}(\mathbf{Q}\mathbf{V}_D\mathbf{Q}) + \text{tr}(\mathbf{V}\Sigma\mathbf{G}_1) + \text{tr}(\Sigma\mathbf{V}\mathbf{G}_1)$
$\text{tr}(\Sigma\mathbf{X}'_D\Sigma\mathbf{X}'^2_D)$	-2	$\text{tr}(\Sigma\mathbf{V}_D\Sigma\mathbf{V}_D^2)$	$2\sum_{x,y=1}^q \text{tr}(\Sigma_{xy}\Sigma_{yx})\text{tr}(\Sigma_{xy}\Sigma_{yx}\mathbf{V}_{xx}) + \text{tr}(\Sigma\mathbf{V}_D\Sigma\mathbf{G}_1)$
$\text{tr}(\Sigma\mathbf{X}'_D\mathbf{X}'\mathbf{X}'_D)$	2	$\text{tr}(\Sigma\mathbf{V}_D\mathbf{V}\mathbf{V}_D)$	$\sum_{x,y=1}^q \text{tr}(\Sigma_{xy}\Sigma_{yx})\text{tr}(\Sigma_{xy}\mathbf{V}_{yx}) + \text{tr}(\Sigma\mathbf{V}_D\Sigma\mathbf{G}_1)$
$\text{tr}(\mathbf{X}'\Sigma\mathbf{X}'^2_D)$	2	$\text{tr}(\mathbf{V}\Sigma\mathbf{V}_D^2)$	$\text{tr}(\mathbf{V}_D\mathbf{G}_5) + (it)\text{tr}((\mathbf{V}\Sigma)_D\mathbf{G}_1) + \text{tr}((\Sigma^2)_D\mathbf{V}_D\mathbf{G}_1)$

where $\mathbf{G} = \text{diag}(\text{tr}(\Psi_{11})\mathbf{I}_{p_1}, \dots, \text{tr}(\Psi_{qq})\mathbf{I}_{p_q})$. Applying (50) again we have

$$\begin{aligned} & \mathbb{E}[q_1(\mathbf{X}) \exp((it)q_0(\mathbf{X}))] \\ &= \exp\left(\frac{(it)^2 \text{tr}(\mathbf{A}^2)}{2}\right) \times \left[d_0 + (it)^2 d_2 \right. \\ & \quad \left. + \frac{1}{\sqrt{n}} \left\{ (it)d_1 + (it)^3 d_3 + (it)^5 d_5 \right\} \right] + \mathcal{O}(n^{-1}), \quad (92) \end{aligned}$$

where

$$d_0 = \text{tr}(\Sigma^2) + \sum_{x,y=1}^q \text{tr}^2(\Sigma_{xy}\Sigma_{yx}) - 2\text{tr}(\Sigma^2\mathbf{G}_1) \quad (93a)$$

$$\begin{aligned} d_1 &= 2\text{tr}(\Sigma)\text{tr}(\mathbf{A}) - 2\text{tr}(\Sigma^2\mathbf{G}_2) - 2\text{tr}(\mathbf{Z}'\mathbf{V}\mathbf{G}_1) - 2\text{tr}(\Sigma\mathbf{G}_1\mathbf{V}_D) \\ & \quad + 2\text{tr}(\mathbf{Z}'\Sigma\mathbf{G}_1\mathbf{V}) + 2\sum_{x,y=1}^q \text{tr}(\Sigma_{xy}\Sigma_{yx})\text{tr}(\mathbf{V}_{xy}\Sigma_{yx}) \quad (93b) \end{aligned}$$

$$\begin{aligned} d_2 &= \text{tr}(\Sigma\mathbf{A}\Sigma\mathbf{A}) - 2\text{tr}(\Sigma(\mathbf{V})_D\mathbf{V}) + \text{tr}(\Sigma\mathbf{V}_D\Sigma\mathbf{V}_D) \\ & \quad - 2\text{tr}(\mathbf{Z}'\mathbf{V}\mathbf{V}_D) + 2\text{tr}(\mathbf{Z}'\mathbf{S}(\mathbf{V}_D)^2) \quad (93c) \end{aligned}$$

$$\begin{aligned} d_3 &= 2\text{tr}(\Sigma\mathbf{A}\Sigma\mathbf{A}^2) + 2\text{tr}(\Sigma\mathbf{V}_D\Sigma\mathbf{P}_D) - 2\text{tr}(\Sigma\mathbf{V}_D\mathbf{P}) \\ & \quad - 2\text{tr}(\Sigma\mathbf{P}_D\mathbf{V}) - 2\text{tr}(\mathbf{Z}'\mathbf{P}\mathbf{V}_D) - 2\text{tr}(\mathbf{Z}'\mathbf{V}\mathbf{P}_D) \\ & \quad + 2\text{tr}(\mathbf{Z}'\Sigma\mathbf{P}_D\mathbf{V}_D) + 2\text{tr}(\mathbf{Z}'\Sigma\mathbf{V}_D\mathbf{P}_D) \quad (93d) \end{aligned}$$

$$\begin{aligned} d_5 &= \frac{\text{tr}(\mathbf{A}^3)}{3} \left[\text{tr}(\Sigma\mathbf{A}\Sigma\mathbf{A}) - 2\text{tr}(\Sigma\mathbf{V}_D\mathbf{V}) + \text{tr}(\Sigma\mathbf{V}_D\Sigma\mathbf{V}_D) \right. \\ & \quad \left. - 2\text{tr}(\mathbf{Z}'\mathbf{V}\mathbf{V}_D) + 2\text{tr}(\mathbf{Z}'\mathbf{S}(\mathbf{V}_D)^2) \right] \quad (93e) \end{aligned}$$

with $\mathbf{V} = \mathbf{Q}\mathbf{A}\mathbf{Q}$, $\mathbf{P} = \mathbf{Q}\mathbf{A}^2\mathbf{Q}$, $\mathbf{G}_1 = \text{diag}(p_1\mathbf{I}_{p_1}, \dots, p_q\mathbf{I}_{p_q})$ and $\mathbf{G}_2 = \text{diag}(\text{tr}(\mathbf{V}_{11})\mathbf{I}_{p_1}, \dots, \text{tr}(\mathbf{V}_{qq})\mathbf{I}_{p_q})$.

On the other hand, the mathematical expectations in (54) can be obtained in an identical manner as (83), which are given in Tables V and VI. Here we have $\mathbf{G}_3 = \text{diag}(\text{tr}((\mathbf{Z}'\mathbf{Z})_{11})\mathbf{I}_{p_1}, \dots, \text{tr}((\mathbf{Z}'\mathbf{Z})_{qq})\mathbf{I}_{p_q})$, $\mathbf{G}_4 = \text{diag}(\text{tr}((\mathbf{Q}\mathbf{Z}'\mathbf{Q})_{11})\mathbf{I}_{p_1}, \dots, \text{tr}((\mathbf{Q}\mathbf{Z}'\mathbf{Q})_{qq})\mathbf{I}_{p_q})$ and $\mathbf{G}_5 = \text{diag}(\text{tr}((\mathbf{\Sigma}^2)_{11})\mathbf{I}_{p_1}, \dots, \text{tr}((\mathbf{\Sigma}^2)_{qq})\mathbf{I}_{p_q})$.

REFERENCES

- [1] S. S. Wilks, "Certain generalizations in the analysis of variance," *Biometrika*, vol. 24, nos. 3–4, pp. 471–494, 1932.
- [2] K. C. S. Pillai, *Statistical Tables for Tests of Multivariate Hypotheses*. Manila, Philippines: Statistical Center, Univ. Philippines, 1960.
- [3] K. C. S. Pillai, "Some new test criteria in multivariate analysis," *Ann. Math. Statist.*, vol. 26, no. 1, pp. 117–121, 1955.
- [4] S. N. Roy, "The individual sampling distribution of the maximum, the minimum and any intermediate of the p -statistics on the null-hypothesis," *Sankhyā, Indian J. Statist.*, vol. 7, no. 2, pp. 133–158, 1945.
- [5] S. S. Wilks, "On the independence of k sets of normally distributed statistical variables," *Econometrica*, vol. 3, no. 3, pp. 309–326, 1935.
- [6] J. K. Tugnait, "On multiple antenna spectrum sensing under noise variance uncertainty and flat fading," *IEEE Trans. Signal Process.*, vol. 60, no. 4, pp. 1823–1832, Apr. 2012.
- [7] D. Ramirez, G. Vazquez-Vilar, R. López-Valcarce, J. Via, and I. Santamaria, "Detection of rank- P signals in cognitive radio networks with uncalibrated multiple antennas," *IEEE Trans. Signal Process.*, vol. 59, no. 8, pp. 3764–3774, Aug. 2011.
- [8] A. Mariani, A. Giorgetti, and M. Chiani, "Test of independence for cooperative spectrum sensing with uncalibrated receivers," in *Proc. IEEE Global Commun. Conf. (GLOBECOM)*, Dec. 2012, pp. 1374–1379.
- [9] D. Ramirez, J. Via, I. Santamaria, and L. L. Scharf, "Detection of spatially correlated Gaussian time series," *IEEE Trans. Signal Process.*, vol. 58, no. 10, pp. 5006–5015, Oct. 2010.
- [10] A. Leshem and A.-J. van der Veen, "Multichannel detection and spatial signature estimation with uncalibrated receivers," in *Proc. 11th IEEE Workshop Statist. Signal Process.*, Singapore, Dec. 2001, pp. 190–193.
- [11] L. L. Scharf and J. K. Thomas, "Wiener filters in canonical coordinates for transform coding, filtering, and quantizing," *IEEE Trans. Signal Process.*, vol. 46, no. 3, pp. 647–654, Mar. 1998.
- [12] H.-S. Chen and W. Gao, "Spectrum sensing for TV white space in North America," *IEEE J. Sel. Areas Commun.*, vol. 29, no. 2, pp. 316–326, Feb. 2011.
- [13] H. Nagao, "On some test criteria for covariance matrix," *Ann. Statist.*, vol. 1, no. 4, pp. 700–709, 1973.
- [14] D. Ramirez, J. Via, I. Santamaria, and L. L. Scharf, "Locally most powerful invariant tests for correlation and sphericity of Gaussian vectors," *IEEE Trans. Inf. Theory*, vol. 59, no. 4, pp. 2128–2141, Apr. 2013.
- [15] T. Adali, P. J. Schreier, and L. L. Scharf, "Complex-valued signal processing: The proper way to deal with impropriety," *IEEE Trans. Signal Process.*, vol. 59, no. 11, pp. 5101–5125, Nov. 2011.
- [16] N. Sugiura, "Asymptotic non-null distributions of the likelihood ratio criteria for covariance matrix under local alternatives," *Ann. Statist.*, vol. 1, no. 4, pp. 718–728, 1973.
- [17] H. Nagao, "Asymptotic nonnull distributions of certain test criteria for a covariance matrix," *J. Multivariate Anal.*, vol. 4, no. 4, pp. 409–418, 1974.
- [18] H. Nagao, "Nonnull distributions of two test criteria for independence under local alternatives," *J. Multivariate Anal.*, vol. 3, no. 4, pp. 435–444, 1973.
- [19] X. Mestre, P. Vallet, and W. Hachem, "Asymptotic analysis of linear spectral statistics of the sample coherence matrix," in *Proc. IEEE Int. Conf. Acoust., Speech, Signal Process. (ICASSP)*, Brisbane, Australia, Apr. 2015, pp. 5679–5683.
- [20] S. M. Kay, *Fundamentals of Statistical Signal Processing: Detection Theory*, vol. 2. Englewood Cliffs, NJ, USA: Prentice-Hall, 1998.
- [21] N. R. Goodman, "Statistical analysis based on a certain multivariate complex Gaussian distribution (an introduction)," *Ann. Math. Statist.*, vol. 34, no. 1, pp. 152–177, 1963.
- [22] Y. Fujikoshi, "Asymptotic expansions of the distributions of test statistics in multivariate analysis," *J. Sci. Hiroshima Univ. Ser. A-I*, vol. 34, no. 1, pp. 144–173, 1970.
- [23] A. C. Berry, "The accuracy of the Gaussian approximation to the sum of independent variables," *Trans. Amer. Math. Soc.*, vol. 49, no. 1, pp. 122–126, 1941.
- [24] C.-G. Esseen, "On the Liapounoff limit of error in the theory of probability," *Arkiv Matematik, Astronomi Fysik*, vol. 28A, no. 9, pp. 1–19, 1942.
- [25] T. W. Anderson, "On the distribution of the two-sample Cramér-von Mises criterion," *Ann. Math. Statist.*, vol. 33, no. 3, pp. 1148–1159, 1962.
- [26] H. Jack, "Jacobians of transformations involving orthogonal matrices," *Proc. Roy. Soc. Edinburgh Sec. A, Math.*, vol. 67, no. 2, pp. 81–103, 1965.
- [27] G. Stewart, *Matrix Algorithms (Basic Decompositions)*, vol. 1. Cambridge, U.K.: Cambridge Univ. Press, 1998.
- [28] G. Marsaglia and J. C. W. Marsaglia, "A new derivation of Stirling's approximation to $n!$," *Amer. Math.*, vol. 97, no. 9, pp. 826–829, 1990.

Yu-Hang Xiao was born in Anhui on January 20, 1992. He received the B.E. degree in microelectronics from Harbin Engineering University, Harbin, China, and M.E. degree in information and communication engineering from Harbin Institute of Technology (HIT), Harbin, China, in 2012 and 2014, respectively. Since September 2014, he has been pursuing the Ph.D. degree in the field of information and communication engineering at HIT. He is currently a joint Ph.D. studying in Department of Electrical and Computer Engineering, McMaster University, Hamilton, ON, Canada. His research interests are in statistical signal processing and MIMO communications.

Lei Huang (M'07–SM'14) was born in Guangdong, China. He received the B.Sc., M.Sc., and Ph.D. degrees in electronic engineering from Xidian University, Xian, China, in 2000, 2003, and 2005, respectively.

From 2005 to 2006, he was a Research Associate with the Department of Electrical and Computer Engineering, Duke University, Durham, NC. From 2009 to 2010, he was a Research Fellow with the Department of Electronic Engineering, City University of Hong Kong and a Research Associate with the Department of Electronic Engineering, The Chinese University of Hong Kong. From 2011 to 2014, he was a Professor with the Department of Electronic and Information Engineering, Harbin Institute of Technology Shenzhen Graduate School. Since November 2014, he has joined the College of Information Engineering, Shenzhen University, where he is currently a Distinguished Professor. His research interests include array signal processing, statistical signal processing, sparse signal processing and their applications in radar, navigation and wireless communications.

He is currently serving as an Associate Editor for IEEE TRANSACTIONS ON SIGNAL PROCESSING and the *Digital Signal Processing*. Additionally, he is an elected member in Sensor Array and Multichannel (SAM) Technical Committee (TC) of the IEEE Signal Processing Society.

Junhao Xie (M'02–SM'14) received the B.S. degree in electronic engineering from Harbin Institute of Shipbuilding Engineering, the M.S. degree in signal and information processing from Harbin Engineering University and the Ph.D. degree in communication and information system from Harbin Institute of Technology, in 1992, 1995 and 2001 respectively.

From 2004 to 2006, he was a visiting scholar at Curtin University of Technology, Perth, W.A., Australia, where he dealt with radar remote sensing signal processing. He is a Professor in the Department of Electronic Engineering, Harbin Institute of Technology. His past and present research interests involve radar system analysis and modeling, array signal processing, target detection and estimation, and ocean remote sensing for shipborne highfrequency surface wave radar (HFSWR) and inverse synthetic aperture radar (ISAR).

Hing Cheung So (S'90–M'95–SM'07–F'15) was born in Hong Kong. He received the B.Eng. degree from the City University of Hong Kong and the Ph.D. degree from The Chinese University of Hong Kong, both in electronic engineering, in 1990 and 1995, respectively. From 1990 to 1991, he was an Electronic Engineer with the Research and Development Division, Everex Systems Engineering Ltd., Hong Kong. During 1995–1996, he was a Postdoctoral Fellow with The Chinese University of Hong Kong. From 1996 to 1999, he was a Research Assistant Professor with the Department of Electronic Engineering, City University of Hong Kong, where he is currently a Professor. His research interests include detection and estimation, fast and adaptive algorithms, multidimensional harmonic retrieval, robust signal processing, source localization, and sparse approximation.

He has been on the editorial boards of *IEEE Signal Processing Magazine* (2014–), *IEEE TRANSACTIONS ON SIGNAL PROCESSING* (2010–2014), *Signal Processing* (2010–), and *Digital Signal Processing* (2011–). He is also Lead Guest Editor for *IEEE JOURNAL OF SELECTED TOPICS IN SIGNAL PROCESSING*, special issue on “Advances in Time/Frequency Modulated Array Signal Processing.” In addition, he was an elected member in Signal Processing Theory and Methods Technical Committee (2011–2016) of the IEEE Signal Processing Society where he was chair in the awards subcommittee (2015–2016).